CHAPTER 10

Climate Effects of Ozone and Halocarbon Changes

Lead Authors:
C. Granier
K.P. Shine

Coauthors:
J.S. Daniel
J.E. Hansen
S. Lal
F. Stordal

Contributors:
S. Bekki
L. Bishop
J.S. Fuglestvedt
J.-E. Jonson
S. Madronich
G. Myhre

CHAPTER 10

CLIMATE EFFECTS OF OZONE AND HALOCARBON CHANGES

Contents

SCIENTIFIC SUMMARY

- **Increased penetration of UV radiation to the troposphere as a result of stratospheric ozone depletion leads to changes in key photochemical processes in the troposphere.** Model simulations have been used to estimate that a 1% decrease in global total ozone leads to a global increase of about 1.5% in the photolytic production of the first excited state of atomic oxygen, $O(^1D)$, from ozone. This results in a 0.7 to 1% increase in globally averaged tropospheric hydroxyl radical (OH). Since OH is the main oxidant for climatically important gases, such as methane (CH_4), hydrochlorofluorocarbons (HCFCs), and hydrofluorocarbons (HFCs), this change would be expected to decrease their lifetimes. Stratospheric ozone depletion may have contributed 20 to 40% of the reduction in CH_4 growth rate, and 25 to 40% of the carbon monoxide (CO) surface concentration decrease during the two years following the Mt. Pinatubo volcanic eruption in 1991. The effect on those species whose lifetimes depend on OH has not yet been quantified.

- **The first systematic calculations of the effects of ozone changes on climate using a general circulation model (GCM) have been reported.** Previous assessments highlighted the climatic importance of ozone changes near the tropopause. When taking into account the impact of ozone changes on cloudiness, this GCM study suggests that changes in lower tropospheric ozone are of similar importance to changes near the tropopause. This study suggests that, because of the cloud interactions, the ozone change since the late 1970s may have resulted in a surface temperature change 20-30% smaller than that implied by radiative forcing. Given the known difficulties in modeling cloud processes in GCMs, the generality of conclusions drawn from a single model must be treated with caution.

- **The global-average radiative forcing due to changes in stratospheric ozone since the late 1970s is estimated to be -0.2 ± 0.15 Wm^{-2}.** The central value of this forcing estimate is about double the Intergovernmental Panel on Climate Change (IPCC, 1996) estimate, partly because the calculations now include the increased ozone losses during the 1990s. There remain uncertainties due to difficulties in defining the vertical profile of ozone change and in calculating the stratospheric temperature response to this change. The stratospheric ozone forcing may have offset about 30% of the forcing due to the increases in the well-mixed greenhouse gases since the late 1970s.

- **Recovery of stratospheric ozone would reduce the offset to the radiative forcing of the other greenhouse gases.** The ozone recovery will therefore lead to a more rapid increase in radiative forcing than would have occurred due to increases in other greenhouse gases alone.

- **The global-average radiative forcing due to increases in tropospheric ozone since preindustrial times is estimated to be $+0.35 \pm 0.15$ Wm^{-2}.** This estimate is consistent with the IPCC (1996) estimate of 0.4 ± 0.2 Wm^{-2}, but is based on a much wider range of model studies; significant uncertainties remain because of inter-model differences and the lack of data for evaluating the model results. Since the forcing due to the increases in "well-mixed" greenhouse gases since preindustrial times is about 2.5 Wm^{-2}, the tropospheric ozone changes may have enhanced this forcing by 10-20%.

- **Coupled ocean-atmosphere GCMs have been used to calculate the impact of stratospheric ozone loss on the thermal structure of the atmosphere.** The observed stratospheric ozone depletion appears to explain much of the observed temperature decrease in the lower stratosphere. The calculated altitude of the transition from tropospheric warming to stratospheric cooling is in better agreement with observations when ozone depletion is taken into account. The global average surface temperature is estimated to be about 0.1°C cooler over the past two decades as a result of the stratospheric ozone loss; this can be compared with the calculated warming of about 0.3°C over the same period, due to well-mixed greenhouse gas increases.

- **The CFC-11 radiative forcing has been revised.** The currently recommended chlorofluorocarbon-11 (CFC-11) radiative forcing is 12% higher than the value used in IPCC (1990) and subsequent assessments. The change is primarily due to the use of an improved vertical profile of CFC-11. Because this gas was used as a reference in previous assessments to calculate the forcing for many other molecules, its change leads to revised radiative forcings recommendations for these gases.

- **Radiative forcings and Global Warming Potentials (GWPs) are presented for an expanded set of gases.** New categories of gases in the radiative forcing set include fluorinated organic molecules. For some of these gases, GWPs are not reliable, because laboratory data are not available for determination of the lifetimes. The direct GWPs have been calculated relative to carbon dioxide (CO_2) using an improved calculation of the CO_2 radiative forcing, the IPCC (1996) response function for a CO_2 pulse, and new values for the radiative forcing and lifetimes for a number of halocarbons. As a consequence of changes in the radiative forcing for CO_2 and CFC-11, the revised GWPs are typically 20% higher than listed in IPCC (1996). Indirect GWPs are also presented. The direct GWPs, for those species whose lifetimes are well characterized, are estimated to be accurate within ±35%, but the indirect GWPs are less certain.

10.1 INTRODUCTION

This chapter reviews our understanding of the links between climate and changes in tropospheric and stratospheric ozone; it also reviews our understanding of the climatic effects of chlorofluorocarbons (CFCs) and related species. Section 10.2 discusses the way that changes in stratospheric ozone can change photolysis rates in the troposphere and consequently the distribution of the hydroxyl radical (OH) and radiatively active species. Section 10.3 describes calculations of the climatic effect of ozone changes using both climate models and the concept of radiative forcing. Section 10.4 discusses the radiative forcing due to CFCs and related species, and includes updated calculations of their Global Warming Potentials (GWPs). Finally, Section 10.5 discusses the relative importance of the climatic effects of ozone changes compared with other climate change mechanisms.

10.2 EFFECTS OF OZONE CHANGE ON RADIATIVELY ACTIVE SPECIES

10.2.1 Effects on Photolysis Rates

The penetration of solar radiation into the troposphere in the ultraviolet-B (UV-B) part of the solar spectrum (280-315 nm) is to a large extent determined by the thickness of the ozone column in the stratosphere. Therefore, as discussed in Chapter 9, the reduction in the total column ozone distribution observed over recent decades has resulted in increases in ultraviolet radiation reaching the troposphere. This could affect some fundamental photochemical processes in the troposphere, because enhanced UV-B radiation in the troposphere increases the photodissociation of some key chemical species. At wavelengths greater than about 320 nm, the absorption by ozone becomes weak, and the intensity of the solar flux is almost entirely determined by atmospheric scattering. Thus, changes in total column ozone affect mainly chemical species that photolyze mostly in the UV-B region.

Similar to the radiation amplification factor used in Chapters 9 and 11, a measure of the sensitivity of photolytic processes to total column ozone can be given by the sensitivity factor S, which is defined as the percentage change in a photodissociation rate J for a percentage change in total column ozone Ω :

$$\frac{\Delta J}{J} = -S\frac{\Delta\Omega}{\Omega} \qquad (10\text{-}1)$$

It should be noted that the sensitivity factor S depends on total column ozone, as well as on the altitude of the ozone perturbation and on the solar zenith angle. Examples of sensitivity factors for several photolysis processes and for different conditions are given in Table 10-1 (Madronich and Granier, 1994; Fuglestvedt *et al.*, 1994; Krol and van Weele, 1997). The photodissociation of ozone is the most sensitive to changes in total column ozone, a 1% decrease in total column ozone resulting in a 1.4 to 2.3% increase in the photodissociation rate in the troposphere, depending on location, time, and spatial and temporal averaging.

Calculations made before 1997 of the sensitivity of ozone photolysis ($O_3 + h\nu \rightarrow O(^1D) + O_2$) to total column ozone assumed a quantum yield for the formation of the first excited state of atomic oxygen ($O(^1D)$) as recommended by DeMore *et al.* (1994). However, recent

Table 10-1. Sensitivity factors *S* for key photolytic processes in the troposphere, as defined in Equation (10-1). The values in the table correspond to near-surface conditions and (1) a total column ozone of 324 DU and a zenith angle of 46˚, (2) a diurnal average for 20˚N, May 15, and a total column ozone of 280 DU, and (3) global annual tropospheric mean value. $J_1(CH_2O)$ and $J_2(CH_2O)$ correspond to reactions ($CH_2O + h\nu \rightarrow H + HCO$) and ($CH_2O + h\nu \rightarrow H_2 + CO$), respectively.

Reference	$J(O_3)$	$J(NO_2)$	$J(H_2O_2)$	$J(HNO_3)$	$J_1(CH_2O)$	$J_2(CH_2O)$
Krol and van Weele (1997) (1)	2.3	0	0.4	1.1	0.5	0.2
Madronich and Granier (1994) (2)	1.83	0.02	0.36	1.08	0.45	0.15
Fuglestvedt *et al.* (1994) (3)	1.4	0.04	0.35	0.89	0.47	0.16

Table 10-2. Sensitivity factor *S*, as defined in Equation (10-1), for $J(O_3 \rightarrow O(^1D))$ for quantum yields recommended by DeMore *et al.*, 1994 ("JPL 1994") and DeMore *et al.*, 1997 ("JPL 1997"). The calculations indicated as Jonson-1997, Madronich-1997, and Granier-1997 have been performed using updated versions of the models used by Fuglestvedt *et al.* (1994), Madronich and Granier (1994), and Granier *et al.* (1996), respectively. Sensitivity factors correspond to tropospheric (1) global annual and (2) monthly mean values.

Calculation	S (JPL 1994)	S (JPL 1997)	Difference
Jonson (1) (1997)	1.56	1.46	-7%
Madronich (2) (1997) summer	2.02	1.69	-16%
Madronich (2) (1997) winter	1.72	1.53	-11%
Granier (1) (1997)	1.62	1.39	-14%

measurements have confirmed experiments performed in the late 1980s (Trolier and Wiesenfeld, 1988; Takahashi *et al.*, 1996; Shetter *et al.*, 1996) that suggested that this quantum yield could be up to a factor of 5 larger than previously recommended by DeMore *et al.* (1994) at wavelengths around 315 nm. Higher quantum yields make the photodissociation process in this part of the spectrum less sensitive to changes in the total column ozone. Hence, the sensitivity factors *S* associated with ozone photolysis calculated with the more recent recommended value of the quantum yield (De More *et al.*, 1997) are smaller by 7 to 16% than previously reported values, as listed in Table 10-2.

10.2.2 Effects on Tropospheric Chemistry

UV-B is one of the key environmental factors controlling tropospheric chemistry, because the distribution of the most efficient oxidizing compound, the OH radical, depends strongly on the available ultraviolet radiation in the troposphere. The abundance of the OH radical regulates the lifetimes of greenhouse gases such as methane (CH_4), hydrochlorofluorocarbons (HCFCs), and hydrofluorocarbons (HFCs), and of other species such as carbon monoxide (CO) and hydrocarbons. In addition, OH plays an important role in tropospheric chemistry because it controls the production of tropospheric ozone, as discussed in Chapter 8.

The impact of stratospheric ozone change on the fate of tropospheric species has been discussed by Liu and Trainer (1988) and Thompson *et al.* (1990), and more recently by Fuglestvedt *et al.* (1994), Bekki *et al.* (1994), Toumi *et al.* (1994), Fuglestvedt *et al.* (1995), Madronich and Granier (1994), Granier *et al.* (1996), and Van Dop and Krol (1996).

The production of the OH radical in the troposphere occurs through the photodissociation of O_3, yielding (O^1D):

$$O_3 + h\nu\ (\lambda \leq 325\ nm) \rightarrow O(^1D) + O_2 \qquad R1$$

Most of the electronically excited oxygen atoms produced through this process are deactivated to produce ground-state $O(^3P)$ atoms. However, a few percent of the $O(^1D)$ atoms react with water vapor to produce OH radicals:

$$H_2O + O(^1D) \rightarrow 2\ OH \qquad R2$$

Reaction R1, as seen in the previous section, is the most sensitive to changes in the overhead O_3 column. Because this process is the main source of OH radicals throughout the troposphere, OH is therefore expected to have increased as a result of the observed depletion in total column ozone over the last decades, if all other factors, such as emissions of CH_4, CO, or nitrogen oxides (NO_x), as well as water vapor distributions, have remained unchanged. The magnitude of the change in OH distribution as a response to changes in $O(^1D)$ is also determined by other chemical processes that could affect OH.

OH radicals react with several chemical species:

$$CO + OH \rightarrow CO_2 + H \quad R3$$
$$CH_4 + OH \rightarrow CH_3 + H_2O \quad R4$$
$$O_3 + OH \rightarrow HO_2 + O_2 \quad R5$$

and with many other gases through analogous reactions.

Rapid cycling is maintained between OH and the hydroperoxyl radical (HO_2) through:

$$HO_2 + O_3 \rightarrow OH + 2\,O_2 \quad R6$$

in remote unpolluted areas, and by

$$HO_2 + NO \rightarrow OH + NO_2 \quad R7$$

when the concentration of nitrogen oxides is larger than about 15-20 parts per trillion by volume (pptv; see discussion in WMO (1992)).

Reactions (R1 + R2) represent, together with R5 and R6, the major loss process of odd oxygen compounds in the troposphere, while R7 corresponds to a production of ozone because NO_2 is a source of oxygen atoms through

$$NO_2 + h\nu\ (\lambda \leq 420\ nm) \rightarrow NO + O \quad R8$$

followed by

$$O + O_2 + M \rightarrow O_3 + M \quad R9$$

where M is a third body such as molecular nitrogen (N_2) or oxygen (O_2). The strong coupling between hydrogen radicals OH and HO_2 is of great importance for the evaluation of perturbations of the OH distribution, since a major part of the loss of odd hydrogen (HO_x) in the free troposphere proceeds via reactions involving both radicals. In regions of low nitrogen oxides, loss of odd hydrogen radicals results from reaction

$$OH + HO_2 \rightarrow H_2O + O_2 \quad R10$$

or through the sequence

$$HO_2 + HO_2 \rightarrow H_2O_2 + O_2 \quad R11$$
$$H_2O_2 + OH \rightarrow H_2O + HO_2 \quad R12$$

H_2O_2 is also removed through washout or by dry deposition.

When the concentrations of nitrogen oxides are sufficiently high, loss of odd hydrogen results from reactions

$$OH + NO_2 + M \rightarrow HNO_3 + M \quad R13$$

and

$$OH + HNO_3 \rightarrow H_2O + NO_3 \quad R14$$

The chemical processes described above are responsible for the strong dependence of concentrations of OH and other radicals on CH_4, CO, and NO_x levels.

Different types of photochemical models and chemical transport models (CTMs) have been used to assess the impact of the observed total column ozone changes on tropospheric composition at the global scale (Bekki *et al.*, 1994; Fuglestvedt *et al.*, 1995; Madronich and Granier, 1994; Granier *et al.*, 1996; and Van Dop and Krol, 1996). These models have been used to calculate the sensitivity, α, of the distribution of tropospheric OH and other tropospheric chemical species to total column ozone changes, defined as (Fuglestvedt *et al.*, 1994)

$$\alpha(X) = -\frac{\left(\frac{\Delta X}{X}\right)}{\left(\frac{\Delta \Omega}{\Omega}\right)} \quad (10\text{-}2)$$

where X represents the global tropospheric annual average level of $J(O_3 \rightarrow O(^1D))$, OH, O_3, and CH_4; and Ω is the total column ozone. Ω and X represent the reference level, while $\Delta\Omega$ and ΔX represent the difference between the perturbed level and the reference level. The values of the sensitivities α obtained by the different two- and three-dimensional models, calculated for total column ozone changes observed during the 1979-1994 period, are reported in Table 10-3.

The fact that $\alpha(OH)$ is lower than $\alpha(J(O_3))$ indicates that mechanisms exist that damp the perturbations. The response of chemical species distribution to total column ozone changes is not uniform in space and depends significantly on the distribution of nitrogen oxides. The model results show OH concentrations increase for all NO_x levels, and that OH has a higher sensitivity to total column ozone changes for lower NO_x.

Higher levels of OH lead also to enhancements of HO_2 concentrations, which lead to a further decrease in

Table 10-3. Sensitivity of the ozone photodissociation rates and of tropospheric chemical species to stratospheric ozone changes for the period 1979-1994, as defined in Equation (10-2). The values reported here correspond to the relative change in global tropospheric annual average levels in *X* (%) resulting from a 1% decrease in total column ozone; the assumed scenarios are discussed in the cited publications. The type of model used is indicated in parentheses. Note that the values of Granier *et al.* (1996) correspond to the 1990-1994 period. The calculations indicated as Granier-1997 correspond to the 1979-1994 period and have been obtained using an updated version of the model used by Granier *et al.* (1996).

Reference	X=J(O_3)	X=OH	X=O_3 trop	X=CH_4
Bekki *et al.* (1994) (2-D)	N/A	0.86	N/A	N/A
Fuglestvedt *et al.* (1994) (2-D)	1.38	0.99	-0.29	-0.79
Van Dop and Krol (1996) (1-D)	N/A	0.45*X(J(O_3))	N/A	N/A
Granier *et al.* (1996) (3-D)	1.57	0.82	-0.32	N/A
Granier-1997 (3-D JPL94)	1.39	0.70	-0.27	N/A
Granier-1997 (3-D JPL97)	1.27	0.74	-0.29	N/A

tropospheric ozone through reactions R5 and R6. In regions where low levels of nitrogen oxides are found, the loss of ozone through R1 and R2 will also contribute to the reduction of ozone concentrations. The 2-D and 3-D models calculate a global decrease in tropospheric ozone as a result of decreasing stratospheric ozone. However, whereas the 3-D intermediate model of the annual and global evolution of species (IMAGES; Granier *et al.*, 1996) calculates a decrease in ozone at all latitudes and times of year, the 2-D model of Fuglestvedt *et al.* (1994) calculates a global ozone decrease, except for spring at mid- and high latitudes of the Northern Hemisphere, where an ozone increase is calculated. In this model, ozone precursors accumulate during winter, and when the UV radiation increases in spring, the chemical activity increases strongly, thereby affecting the ozone chemistry, leading to ozone net production for a period. In the perturbed case, the chemical activity starts earlier in the spring than in the unperturbed case. The difference between these results obtained by a 2-D and a 3-D model could be due to different spatial resolution, different parameterization of the chemical scheme involving nonmethane hydrocarbons (NMHCs), or lower nitrogen oxides concentrations calculated by the IMAGES model, making the role of reaction R7 less important than in the Fuglestvedt *et al.* (1994) study.

Two sets of 3-D model calculations were performed using the values of the J($O_3 \rightarrow O(^1D)$) quantum yields from DeMore *et al.* (1994) and DeMore *et al.* (1997) with an updated version of the IMAGES model (Granier *et al.*, 1996); the calculated values for the α sensitivity factor are reported in Table 10-3. Though the sensitivity of J(O_3) is larger for the lower quantum yields reported in DeMore *et al.* (1994), the sensitivity of OH and tropospheric O_3 to total column ozone are slightly lower and higher, respectively, for quantum yields reported in DeMore *et al.* (1997). This may be due to the fact that absolute J($O_3 \rightarrow O(^1D)$) values and OH concentrations are higher in the latter case, resulting in a marginal global decrease in nitrogen oxides. It should be mentioned however that such results could be model-dependent and need to be confirmed by other model evaluations.

10.2.3 Changes in Greenhouse Gases and Ozone Precursor Budgets and Lifetimes Since 1979

The removal of most tropospheric trace gases, including CO and greenhouse gases like methane, HCFCs, and HFCs, is dominated by the reaction with OH. Therefore, any changes in tropospheric OH resulting from stratospheric ozone changes should be accompanied by changes in the growth rates of these trace gases. Furthermore, the atmospheric levels of CO and CH_4 are closely linked to their interaction with OH, because

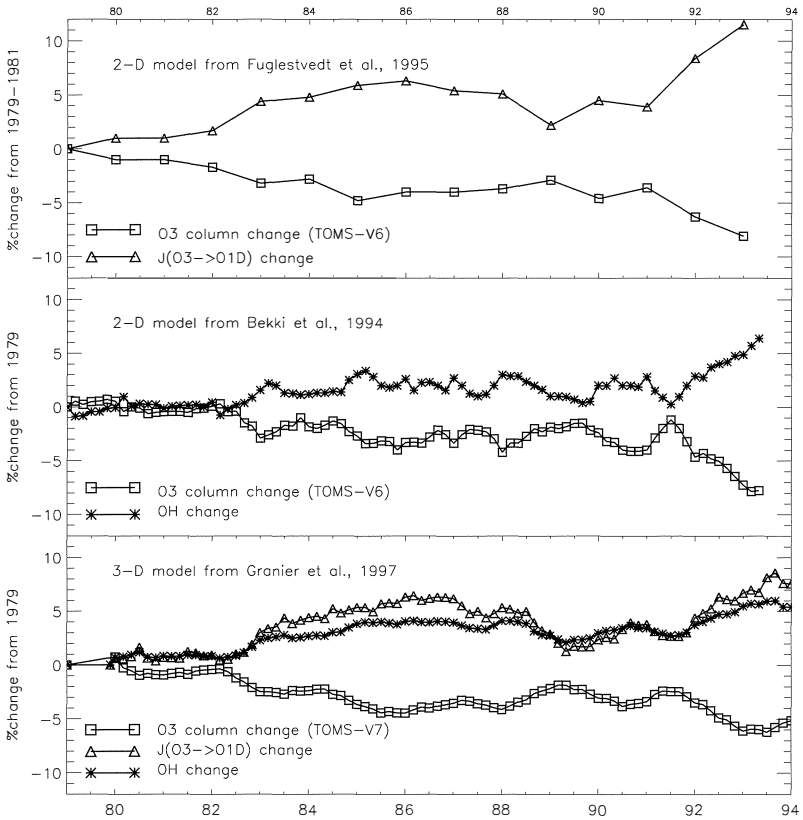

Figure 10-1. Relative change in total column ozone and calculated associated change in $J(O_3 \rightarrow O^1D)$ rate (top; from Fuglestvedt *et al.*, 1995), global tropospheric OH (middle; from Bekki *et al.*, 1994), and $J(O_3 \rightarrow O^1D)$ rate and global OH (bottom; from updated version of Granier *et al.*, 1996 (C. Granier, NOAA Aeronomy Laboratory, U.S., personal communication, 1997)).

changes in the emissions of CO may affect the levels and lifetime of CH_4, or vice versa, through induced changes in the global OH distribution. This section focuses on the impact of stratospheric ozone depletion on the evolution of tropospheric species; the impact of surface emissions changes is discussed in Chapter 8.

As discussed in Chapter 2, surface measurements from global networks have revealed a decline in the growth rate of CH_4 during the last decades, from 17-21 parts per billion by volume (ppbv) per year in the early 1980s to 12-14 ppbv/yr at the end of the 1980s. Measurements performed over the last few years indicate a growth rate of about 6 ppbv/yr in 1995-1996. Most of this reduction has been occurring in the Northern Hemisphere. The methane growth rate slowed down even more during the 1991-1993 period and showed a value between zero and 5 ppbv/yr at the end of 1992 (Dlugokencky *et al.*, 1994). Concentrations of CO, after showing a positive trend until the late 1980s, were characterized by a significant decrease from 1990 to 1993. A decrease of 7 ppbv/yr was observed in the Northern Hemisphere and 4 ppbv/yr in the Southern Hemisphere (Novelli *et al.*, 1994).

The 2-D models of Bekki *et al.* (1994) and Fuglestvedt *et al.* (1995) have calculated the change in the global tropospheric OH and O_3 distributions as well as the change in the CH_4 and CO trends resulting from stratospheric ozone decrease since the early 1980s. The 3-D IMAGES model (Granier *et al.*, 1996) has also been used to calculate changes in the global distributions of OH and O_3 over the 1979-1994 period. In these simulations, the total column ozone from Total Ozone Mapping Spectrometer (TOMS) measurements was used as an input for calculations of the photodissociation rates. Starting in June 1979 until the end of 1992, TOMS Nimbus-7 observations were used; an average of Nimbus-7 and Meteor-3 observations was used for the first four months of 1993; and Meteor-3 observations were used for the remainder of 1993 and the first months of 1994. Model studies performed before 1995 used Version 6 of TOMS measurements; the more recent simulations used Version 7 of the data.

Results from the different simulations are shown in Figure 10-1. Bekki *et al.* (1994) calculated an increase

in global tropospheric OH of 0.3%/yr between 1979 and 1990, followed by a maximum increase of 6% from mid-1991 to spring 1993, with their 2-D model; these are similar to the values obtained with an updated version of the 3-D model used by Granier *et al.* (1996). This latter increase was smaller in the Southern Hemisphere (5%) than in the Northern Hemisphere (8%). Evaluations of trends in the global OH distribution using surface observations of methyl chloroform (CH_3CCl_3) have been reported by Prinn *et al.* (1995) and Krol *et al.* (1998). As discussed in Chapter 8, two different statistical methods were used by the authors, who evaluated the OH trend to be close to zero (Prinn *et al.*, 1995) and 0.46 ± 0.6 %/yr (Krol *et al.*, 1998) for the 1979-1993 period. The trend in OH computed by the models is consistent with the evaluation of Krol *et al.* (1998), but more studies are needed before definite quantitative conclusions can be drawn about the magnitude and origin of an OH trend since 1979.

The response in CH_4 due to the increase in OH follows rather well the long-term variation of global ozone. Bekki *et al.* (1994) have calculated a CH_4 growth rate decrease reaching 3 ppbv/yr in 1985, with a maximum decrease of 7 ppbv/yr in the Northern Hemisphere in late 1992. This value, coincident with the record-low total column ozone value observed during this last period, represents about half of the observed decrease in the methane trend. Fuglestvedt *et al.* (1995) calculated a reduction of the methane growth rate of 2-4 ppbv/yr in the mid-1980s and a maximum reduction of 7 ppbv/yr during 1993-1994; their calculations give somewhat higher reductions in the growth rate at high northern latitudes than elsewhere. From recent model simulations, Lelieveld *et al.* (1998) attribute about 20% of the methane trend change over the 1992-1993 period to stratospheric ozone depletion. The reaction rate constant for the methane oxidation by OH (reaction R4) increases with temperature. Therefore, the chemical loss of methane is larger in the lower troposphere at lower latitudes than in the regions where the relative OH changes are largest, i.e., at higher latitudes in the spring months. The low correlation between the changes in OH and the rate of CH_4 oxidation explains this moderate response in methane calculated by the models.

Trends in surface CO also appear to be affected by stratospheric ozone changes. For example, Bekki *et al.* (1994) calculated a decrease of 5-6 ppbv in surface CO from spring 1991 to spring 1993, whereas Granier *et al.* (1996) calculated a decrease in CO concentrations reaching 2-4 ppbv in late 1992/early 1993, in good agreement with the values calculated by Fuglestvedt *et al.* (1994). This significant change calculated after 1991 represents up to about 25-40% of the observed CO trend, which suggests that increases in UV radiation resulting from stratospheric ozone depletion seem likely to have contributed to the observed changes in CH_4 and CO trends, though they cannot entirely explain these changes.

Furthermore, as indicated by Fuglestvedt *et al.* (1994), due to the differences in lifetimes of CH_4 (8 years) and of CO and O_3 (2 to 3 months), large differences in the timing of the responses to changes in total column ozone are expected. Global levels of ozone and CO respond in the same years as changes in total column ozone, with a maximum delay of a few weeks, whereas, due to its longer lifetime, the maximum response of CH_4 occurs with a delay of a few years.

Observations at the South Pole indicate a 17% reduction in surface ozone from December to January over the 1976-1990 period (Schnell *et al.*, 1991). Several explanations were discussed by the authors, who suggest that enhanced net destruction of ozone resulting from the large stratospheric ozone losses in that region is the principal mechanism. Calculations performed by Fuglestvedt *et al.* (1995) give reductions in Antarctic tropospheric ozone of the same magnitude between 1979 and 1993. As indicated in Chapter 8, due to the high variability of tropospheric ozone and the sparsity of trend data, especially in the Southern Hemisphere, comparisons between the calculated impact of stratospheric ozone depletion on tropospheric ozone and observed trends cannot yet be done with confidence.

The trends of several other source gases that are mainly destroyed through reaction with OH could also be affected. For example, Bekki *et al.* (1994) calculated that the growth rate of CH_3CCl_3 should have decreased by 1 pptv/yr from spring 1991 to autumn 1992 as a result of stratospheric ozone depletion. This feedback between stratospheric ozone and halocarbon lifetimes may need to be taken into account when assessing Ozone Depletion Potentials (ODPs) and Global Warming Potentials (GWPs) of species destroyed by OH in the troposphere.

Another species that could be affected by the stratospheric ozone decrease is hydrogen peroxide (H_2O_2), which acts as another important oxidant in the troposphere. Increased UV-B in the troposphere should result in a slight increase in its loss from

photodissociation (Table 10-1); however, the increase in OH and HO_2 due to ozone depletion leads to a larger production of H_2O_2, which eventually results in an increase in H_2O_2 concentrations, especially in areas with low nitrogen oxides concentrations, where the predominant removal mechanism of odd hydrogen radicals is the formation of peroxides. The model study of Fuglestvedt *et al.* (1994) indicates that in most regions, H_2O_2 concentration increases as a result of increased UV. Anklin and Bales (1997), as well as Sigg and Neftel (1991), reported an overall increase of 60% in H_2O_2 during the last 150 years from the analysis of H_2O_2 in Greenland firn/ice core records. Most of this increase occurred in the past 20 years, at a rate of 1.6 to 4% per year since 1970. A larger increase was reported by Anklin and Bales for the 1988 to 1993 period; Anklin and Bales (1997) proposed that this increase could be due in part to increasing UV-B radiation and to a combination of changes in tropospheric chemistry.

In summary, the decrease in total column ozone observed over the last two decades resulted in an increase in the UV-B fluxes to the troposphere and is likely to have been accompanied by an increase in the tropospheric concentration of the OH radical. This process may be responsible for perturbations of the tropospheric distributions and lifetimes of chemical species such as CO, O_3, CH_4, H_2O_2, HCFCs, and HFCs. From currently available model results, 25 to 40% of the decrease in the CO mixing ratio and 20 to 40% of the decrease in the methane trend, observed more particularly during the two years following the Mt. Pinatubo eruption, could be attributed to the significant stratospheric ozone depletion observed over this period.

Some critical uncertainties remain in the model calculations discussed in the previous paragraphs, such as the impact of cloudiness and aerosols on the calculation of photodissociation rates, uncertainties related to the transport of chemical species, and uncertainties in the distribution of key chemical species such as nitrogen oxides or water vapor. This section has focused on the impact of UV changes on the evolution of tropospheric species over the past years, but it should be noted that these changes resulting from UV increase have to be superimposed on changes resulting from other processes, such as changes in surface emissions or in stratosphere-troposphere exchanges, discussed in Chapters 8 and 7, respectively. The overall impact of all these changes has not yet been evaluated.

10.3 CLIMATE CHANGE DUE TO OZONE CHANGES

10.3.1 Introduction

Previous reports (*e.g.*, WMO, 1995; IPCC, 1996) have highlighted the potential role that changes in both tropospheric and stratospheric ozone may have in contributing to climate change. This section aims to review our understanding of this area by considering calculations of both radiative forcing and climate model response to ozone changes. One important mechanism by which decreases in lower stratospheric ozone can have an impact on the surface-troposphere climate is via the cooling of the lower stratosphere that results from the ozone loss; this leads to less thermal infrared radiation being emitted down to the troposphere. The observational evidence for such a cooling, and its attribution, is discussed in detail in Chapter 5.

10.3.2 Relationship Between Radiative Forcing and Climate Response

Radiative forcing is a simple measure of the potential impact of climate change mechanisms. It is the perturbation of the surface-troposphere radiation budget (in Wm^{-2}) following a change, for example, in the concentration of ozone or carbon dioxide (CO_2), in the absence of any other change in tropospheric conditions. The background for its use was discussed in detail in IPCC (1995). The global-mean radiative forcing, ΔF, can be approximately related to the global-mean surface temperature change (ΔT_s), if the forcing is applied for a time sufficient for the surface temperature to come to equilibrium, by the relationship

$$\Delta T_s \approx \lambda \Delta F \qquad (10\text{-}3)$$

Here λ is a climate sensitivity parameter whose value depends on the strength of various feedbacks (such as those due to changes in water vapor, snow/sea-ice extent, and cloudiness); its value is found to vary amongst different models from about 0.3 to 1.1 K $(Wm^{-2})^{-1}$. Expression (10-3) is known to hold (in the sense that λ is independent of the forcing mechanism) for 1-D radiative convective models (1DRCMs) and for general circulation models (GCMs) when relatively "simple" radiative forcings (such as changes in carbon dioxide concentration or solar output) are applied.

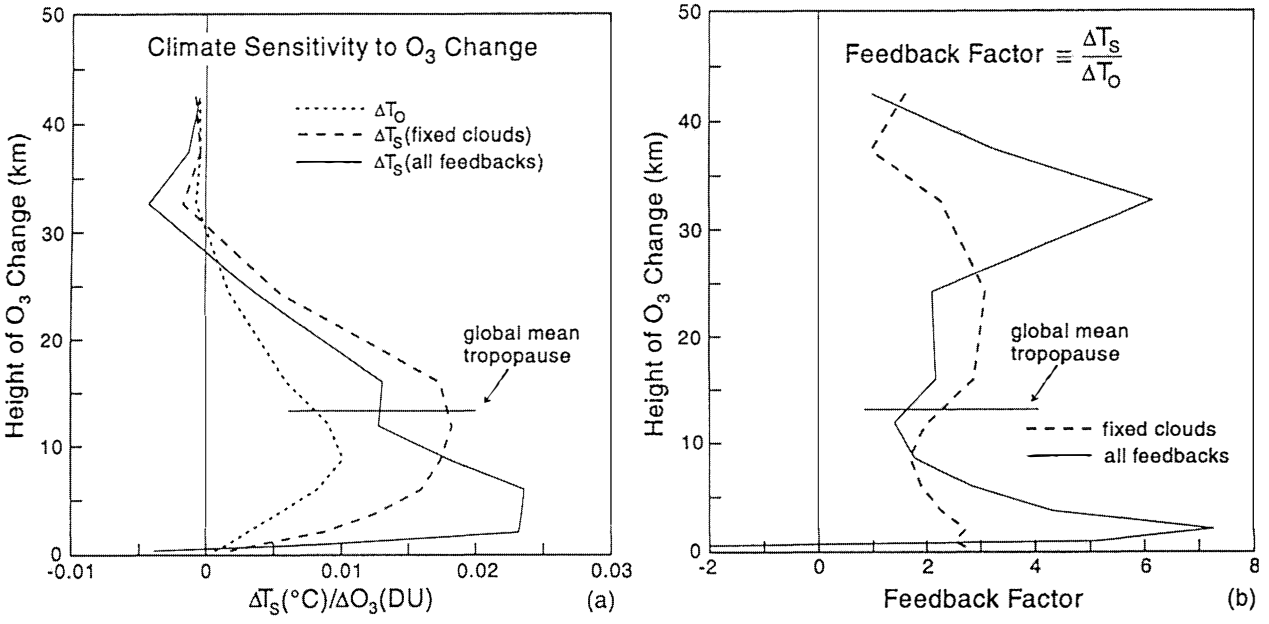

Figure 10-2. (a) Surface air temperature sensitivity of the GISS "Wonderland" GCM to a globally uniform change of 100 DU of atmospheric ozone as a function of the altitude at which the ozone is changed. ΔT_o is the surface temperature response without any climate feedbacks (i.e., clouds, sea ice, water vapor, and tropospheric lapse rate) allowed to operate; ΔT_S is the surface temperature response including feedbacks (either with or without cloud feedbacks). (b) Feedback factor, $\Delta T_S/\Delta T_o$, as a function of the altitude at which the ozone is changed. (From Hansen *et al.*, 1997a.)

Recent GCM experiments have also indicated that, on a global-mean basis, λ is almost independent of forcing mechanism for more complex forcings such as, for example, spatially inhomogeneous sulfate aerosol radiative forcing (Cox *et al.*, 1995) and forcing due to changes in cloud properties (Ramaswamy and Chen, 1997). (There are indications (see below) that the degree to which λ is independent of forcing mechanism depends on whether cloud feedbacks are incorporated in the model; whereas the study of Cox *et al.* (1995) incorporated cloud feedbacks, that of Ramaswamy and Chen (1997) did not.) Haywood *et al.* (1997) have also shown, in transient runs of a coupled ocean-atmosphere GCM, that the climate response to sulfate aerosol and greenhouse gas forcing is approximately equal to the sum of the response to each forcing individually; this additivity applied not only to global-mean changes but also to geographical patterns of surface temperature and precipitation changes.

It must be emphasised that expression (10-3) applies strictly to global-mean changes. Cox *et al.* (1995) and Ramaswamy and Chen (1997) have shown that the regional and even hemispheric-scale response to forcings with the same global-mean magnitude can be quite different. This shows, as noted in IPCC (1995), that even if the global-mean value of ΔF is small, due to a coincidental cancellation of different forcings of opposing signs but different geographical locations, significant sub-global-scale climate changes are still likely.

The most wide-ranging study to date of the relationship between radiative forcing and climate response, and the study of most relevance to the ozone issue, is that of Hansen *et al.* (1997a). They used a simplified version of the Goddard Institute for Space Studies (GISS) GCM that represents the planet as a 120°-longitude sector with nine levels in the vertical. An advantage of this model is that its computational efficiency permitted a larger range of systematic experiments than has hitherto been reported. The generality of the results from this study need to be tested using a range of GCMs, given the known difficulties in modeling cloud processes within GCMs and the relatively crude vertical resolution of this particular model.

Hansen *et al.* (1997a) performed experiments in which ozone was perturbed in each model layer sequentially when the model allowed no feedbacks and when the model included water vapor, sea ice, and tropospheric lapse rate feedbacks, both with cloud feedbacks ("all feedbacks") and without cloud feedbacks ("fixed clouds"). Figure 10-2a shows the surface warming as a function of the height of the ozone perturbation (applied as a constant 100-Dobson unit (DU) perturbation in each layer; the large perturbation was necessary to obtain a clear signal). Figure 10-2b shows the surface temperature response as a function of the height of the ozone perturbation, as a ratio of the "all feedbacks" and "fixed clouds" cases to the no-feedback case; if radiative forcing were an ideal concept, in the sense that λ is independent of the nature of the forcing, then the ratios plotted in Figure 10-2b would be independent of height.

The no-feedback case (Figure 10-2a) shows a peak sensitivity in the upper troposphere/lower stratosphere; the fixed-cloud case generally amplifies the response by a factor of 2, with a reasonably similar shape. These results are qualitatively similar to those from 1DRCM studies of, for example, Wang *et al.* (1980) and Lacis *et al.* (1990), but in the GCM the averaging of latitudes with different tropopause heights and ozone profiles, as well as dynamical mixing, cause the effect of the ozone change to be less strongly peaked at the tropopause. Figure 10-2b shows that in the fixed-cloud case, the feedback factor is approximately independent of the height of the ozone perturbation. However, the inclusion of cloud feedbacks causes a dramatic change in the vertical pattern of the response; in particular, changes in lower tropospheric ozone have a much-heightened sensitivity relative to upper tropospheric changes.

Hansen *et al.* (1997a) also examined the forcing-response relationship using vertical and latitudinal profiles of ozone change based on observations (see also Sections 10.3.3, 10.3.4, and 10.3.5). One measure of the dependence of λ on the forcing mechanism is the ratio of ΔT_s for a particular forcing to ΔT_s for an identical global-mean forcing due to a spectrally uniform change in solar output. With fixed clouds, the ozone forcing caused a 30% greater change in surface temperature than the same global-mean solar forcing, possibly because high-latitude forcings are found to be more effective than low-latitude forcings; with the inclusion of the GISS GCM's cloud feedbacks, however, the ozone forcing causes a 20-30% *smaller* change in surface temperature than the same global-mean solar forcing.

A number of other forcing-response studies have been reported using simpler models. These models lack the detailed interactions between thermodynamic and dynamic processes that are possible in GCMs and so are inherently less suitable for examining the relationship between radiative forcing and climate response; the results must be treated with much more caution. MacKay *et al.* (1997) used a 2-D (latitude-height) model to investigate the climate response to stratospheric ozone loss; their model did not include cloud feedbacks. They found that λ for stratospheric ozone changes is about 3 times higher than it is for carbon dioxide. The difference in sensitivity is much larger than that found in the GCM study of Hansen *et al.* (1997a); for the equivalent experiments, the climate sensitivity was about 20% higher for the ozone loss than for the CO_2 change.

Bintanja *et al.* (1997) used a zonal-average energy balance climate model coupled to a simple zonal-mean ocean model. They explored forcing-response relationships for a range of idealized ozone perturbations in the absence of cloud feedbacks. They concluded that the strength of the ice-albedo feedback is dependent on the meridional distribution of radiative forcing. The feedback, and hence the overall climate response, was strongest when radiative forcings were largest over polar regions; this result is in at least qualitative agreement with the GCM study of Hansen *et al.* (1997a).

Forster *et al.* (1997) used a 1DRCM to investigate the dependence of the forcing-response relationship on the choice of tropopause height (see also Section 10.4.3). In such models, there is a natural choice of tropopause height, being the altitude at which the temperatures change from being in radiative-convective equilibrium to radiative equilibrium. They computed λ using the forcing calculated at this tropopause and at two alternatives, the temperature minimum and the "WMO" tropopause (defined, with elaborations, as the pressure at which the lapse rate falls below 2 K km^{-1}). λ was much less dependent on the nature of the forcing using the top-of-convection tropopause. This indicates that apparent variations in λ in GCM studies may result from an inappropriate choice of tropopause. Unfortunately, in GCMs, as in the real world, it is less easy to define an appropriate tropopause than it is in a 1DRCM.

The overall conclusion of these studies is that radiative forcing remains a useful concept. In the future, if a sufficient consensus develops from similar

experiments with a range of models, it may be possible to develop an "effective" radiative forcing that accounts for the differences in λ amongst different forcing mechanisms. This chapter continues to use radiative forcing, because it seems appropriate for comparing different studies of the same forcing mechanism, and there remains sufficient support from GCM studies to justify its continued use.

10.3.3 Direct Forcing due to Ozone Change

Ozone changes due to human activity are caused by substances that deplete ozone in the stratosphere and by precursors that generate ozone in the troposphere. In addition, to some extent, changes in ozone in the stratosphere can have an impact on ozone in the troposphere, and to a lesser extent vice versa, through stratosphere-troposphere exchange processes (see Chapters 7 and 8). As discussed in WMO (1995) and IPCC (1996), the radiative forcing due to ozone has a longwave as well as a shortwave component and there is a critical dependence on the vertical distribution of ozone changes.

The sensitivity of radiative forcing to the altitude of an ozone change has been discussed in relation to climate sensitivity (Section 10.3.2). Forster and Shine (1997) have used radiative transfer models and observed climatologies of temperatures and clouds to study the relative impact of ozone changes in separate altitude regions. They found, in agreement with the earlier work of Wang *et al.* (1980) and Lacis *et al.* (1990), that the region of largest influence is the tropopause region; but they also pointed to the fact that when relative rather than absolute changes in ozone are considered, the importance of ozone changes in the middle and upper troposphere, as well as the middle stratosphere, is strengthened relative to those near the tropopause. As discussed in Section 10.3.2, Hansen *et al.* (1997a) used a GCM, including all feedbacks (e.g., water vapor, clouds, and surface albedo). They found that, in their model at least, the impact of ozone changes in the mid-to-lower troposphere was much enhanced; they showed that this was mostly due to the impact of the ozone change on cloudiness.

In the stratosphere the temperatures will adjust to a new radiative balance when the ozone distribution is changed. This in turn alters the downwelling of longwave radiation through the tropopause, influencing the radiative forcing there. Radiative forcing taking this effect into account is called *adjusted* forcing, whereas the radiative forcing calculated neglecting the temperature change in the stratosphere is called the *instantaneous* forcing. When temperature changes are taken into account, they are usually calculated assuming that only the radiative balance is changed, and not the dynamical transport of heat in the stratosphere; this is called the fixed dynamical heating approximation. Thorough assessments of the impact of this approximation on the forcing are not yet available. Whereas the earlier work was a mixture of instantaneous and adjusted forcing, the newer work assessed here reports forcing including the temperature adjustment. In Sections 10.3.3.1 and 10.3.3.2, the "direct" radiative forcing (i.e., the forcing due to change in ozone alone) is reported. As discussed in Section 10.2, because ozone photolysis is a primary mechanism controlling the abundance of OH, and because ozone also controls the penetration of ultraviolet radiation, changes in ozone can also alter the concentrations of other radiatively active constituents; the "indirect" forcing due to such changes will be discussed in Section 10.3.4.

10.3.3.1 Stratospheric Ozone

Stratospheric ozone influences the radiative balance by absorption and emission in the longwave as well as absorption in the shortwave region; the two wavelength regions have a different relative importance at different altitudes. A few studies were discussed in WMO (1995) and IPCC (1996): Ramaswamy *et al.* (1992), Hansen *et al.* (1993), Hauglustaine *et al.* (1994), and Molnar *et al.* (1994) all pointed to the strong dependence of the radiative forcing on the vertical distribution of ozone changes. The results were based on observed as well as modeled ozone changes. It was concluded that the radiative forcing due to human-made emissions of ozone-depleting substances was about -0.1 Wm^{-2} with a factor of 2 uncertainty range.

Several new estimates have been made recently and are listed in Table 10-4. Some studies have adopted observed ozone changes, mostly satellite data, and typically report radiative forcing due to ozone changes during the last one or two decades. In Table 10-4 numbers are also given for the forcing per decade, under the assumption that the ozone trend has been linear. This is most likely not the case but is included to allow an easier comparison of the different studies.

Forster and Shine (1997) used an observed climatology of stratospheric temperatures and clouds.

Table 10-4. Radiative forcing due to stratospheric ozone changes. The radiative forcing per decade is also shown to facilitate comparison between calculations based on different time periods; this forcing is derived assuming the trend to be linear in time, which is unlikely to be the case.

Reference	Radiative forcing (Wm^{-2})	Forcing per decade (Wm^{-2})/decade	Time period
Ramaswamy *et al.* (1992)	-0.08	-0.07	1979-1990
Hansen *et al.* (1993)	-0.2	-0.1	1970-1990
Hauglustaine *et al.* (1994)	+0.06	+0.03	1970-1990
Zhong *et al.* (1996)	-0.025	-0.02	1979-1991
Forster and Shine (1997) SAGE	-0.17	-0.10	1979-1996
Forster and Shine (1997) SBUV	-0.22	-0.13	1979-1996
Hansen *et al.* (1997a) SAGE/TOMS	-0.20	-0.13	1979-1994
Hansen *et al.* (1997a) SAGE/SBUV	-0.28	-0.19	1979-1994
Hansen *et al.* (1997b)	-0.3	-0.2	1979-1994
MacKay *et al.* (1997)	-0.06	-0.05	1979-1990
Shine *et al.* (1998)	-0.10	-0.08	1979-1991
Myhre *et al.* (1998a)	+0.05	+0.02	1969-1996

They calculated radiative forcing to be -0.17 and -0.22 Wm^{-2} based on ozone trends from the Stratospheric Aerosol and Gas Experiment (SAGE) and Solar Backscatter Ultraviolet (SBUV) spectrometer, respectively. In the SBUV case only the column data were used, and it was assumed that the ozone loss was limited to a 7-km region above the tropopause. The trends were extrapolated forward to 1996 on the assumption that trends would remain linear. As reported in Chapter 4, this assumption no longer looks justifiable, at least in midlatitudes. The combined effect of the reduced midlatitude trends and the enhanced loss in the Arctic on the radiative forcing has not yet been assessed.

Zhong *et al.* (1996) used observed total ozone change between 1979 and 1991 from TOMS. Like Ramaswamy *et al.* (1992), they distributed the ozone loss in a 7-km region above the tropopause. In contrast to calculating a temperature adjustment, they adopted satellite-observed temperature changes from the Microwave Sounding Unit (MSU). The resulting radiative forcing was -0.024 Wm^{-2}. Shine *et al.* (1998) used the same approach but used temperature changes based on radiosonde data. Unlike Zhong *et al.* (1996), they also included the 14-μm band. The resulting radiative forcing was -0.10 Wm^{-2}. The results of the two calculations must be seen in the perspective that the MSU data have a global coverage but only a limited vertical resolution, whereas the radiosonde temperatures have a better vertical resolution but only a sparse geographical coverage. It is further very important to note that the observed temperature changes can also have causes other than changes in ozone (see Chapter 5).

As discussed in Section 10.3.2, Hansen *et al.* (1997a) and Hansen *et al.* (1997b) used a GCM with a low vertical resolution to study climate effects of ozone changes. Changes in ozone concentration were taken from satellite observations. Their work, which is a pioneering GCM study using realistic ozone changes, also takes into account temperature changes and has the advantage that the temperature changes are dynamically consistent with the ozone changes. The resulting radiative forcing due to stratospheric ozone was -0.20 and -0.28 Wm^{-2} for SAGE/TOMS and SAGE/SBUV, respectively. These results include a change in tropospheric ozone, which cannot easily be separated from the stratospheric component.

MacKay *et al.* (1997) calculated radiative forcing due to stratospheric ozone in a 2-D radiative-dynamical climate model, using observed satellite ozone changes. They calculated temperature changes in their model consistent with this ozone change and arrived at a radiative forcing of -0.06 Wm^{-2}. Their temperatures are

up to 20-30 K too low in certain regions of the lower stratosphere, a fact that may influence their results significantly.

As shown above, several calculations of the radiative forcing due to stratospheric ozone are based on satellite observations. It is worth noting that these results are uncertain (see discussion in Chapter 4 and in WMO (1995)), especially in the near-tropopause region, which is the most important region for the radiative forcing. Myhre *et al.* (1998a) on the other hand used ozone changes calculated in a 2-D chemical transport model (CTM). Their ozone loss was much weaker than in SAGE/SBUV in the lower stratosphere, consistent with ozone changes calculated in other CTMs, which are known to underestimate ozone loss there (see Chapter 7). The resulting change in radiative forcing was slightly positive, namely, +0.05 Wm^{-2}. A stronger ozone loss in the lower stratosphere would lead to a more negative radiative forcing.

On the basis of these newer studies, one can conclude that the radiative forcing due to changes in stratospheric ozone is still uncertain, due to large uncertainties in the vertical distribution of the ozone reductions as well as in temperature changes. Also the impact of recent changes in ozone trends (Chapter 4) has not been assessed. Our best estimate for the radiative forcing since the late 1970s is -0.2 Wm^{-2} with an uncertainty range of ±0.15 Wm^{-2}; this uncertainty range is intended to approximately bracket the majority of published studies and is not a formal indication of uncertainty. In comparison, the best estimate of WMO (1995) and IPCC (1996) was -0.1 Wm^{-2} with a factor of 2 uncertainty. These forcings will be placed in the perspective of other radiative forcings in Section 10.5. It is worth noticing that the future changes in forcing due to stratospheric ozone will depend on the timing and the rate of the recovery of stratospheric ozone (see Chapter 12). If it is assumed that stratospheric ozone loss is near its maximum, the radiative forcing due to stratospheric ozone will not grow much more negative before it starts to get less negative. Thus there will be a decrease in the extent to which stratospheric ozone changes offset the forcing due to the increases in other greenhouse gases (see, e.g., Solomon and Daniel, 1996).

10.3.3.2 Tropospheric Ozone

WMO (1995) and IPCC (1996) reported a large uncertainty in the forcing due to anthropogenically related increases in tropospheric ozone that originate from emissions of ozone precursors: NO_x, CO, CH_4, and nonmethane hydrocarbons. Again the uncertainty is connected to uncertainties in the changes in the ozone distribution; these changes are even less well documented than those of stratospheric ozone, for which at least changes in the total column can be inferred from ground-based and satellite observations. Chapter 8 reviews our understanding of tropospheric ozone and its changes, and associated observations. The calculations of radiative forcing presented here are mostly based on the use of chemical transport models; the ozone fields from these models are difficult to evaluate, particularly for the preindustrial period, because of the scarcity of appropriate observations.

Earlier work assessed in WMO (1995) was based on observations (Fishman, 1991; Marenco *et al.*, 1994) as well as model calculations (e.g., Hauglustaine *et al.*, 1994) of ozone change. Several recent studies, which are considered here, are based mostly on modeled ozone distributions (Table 10-5). When the numbers in Table 10-5 are compared, it should be kept in mind that they are based on a variety of assumptions. For example, not all results include temperature adjustment in the stratosphere and effects of clouds. Neglect of either of these effects has been estimated to lead to an overestimate of radiative forcing by approximately 10-25% (Berntsen *et al.*, 1997). This is because (i) clouds reduce the outgoing longwave radiation and hence also reduce the sensitivity to changes in greenhouse gas concentration and (ii) increases of tropospheric ozone reduce the absorption of radiation by ozone in the lower stratosphere, leading to a stratospheric cooling and reduced emission into the troposphere.

The work of Hansen *et al.* (1997b), already discussed for its stratospheric contribution, is based on GCM runs, but ozone distributions were taken from the model of the general universal tracer transport in the atmosphere (MOGUNTIA) 3-D CTM (Crutzen, 1994). The radiative forcing due to increases in tropospheric ozone since preindustrial time was estimated to be 0.3 Wm^{-2}. The MOGUNTIA model was also used by van Dorland *et al.* (1997), who calculated the radiative forcing to be 0.38 Wm^{-2}.

Chalita *et al.* (1996) used a similar approach to that of Hansen *et al.* (1997b), using ozone distributions from a 3-D CTM (IMAGES) to study climate impacts in a GCM. They reported a radiative forcing of 0.28 Wm^{-2} due to an increase in tropospheric ozone. Temperature

Table 10-5. Radiative forcing due to tropospheric ozone changes, all since preindustrial times.

Reference	Radiative forcing (Wm^{-2})
Marenco *et al.* (1994)	0.62
Hauglustaine *et al.* (1994)	0.55
Lelieveld and van Dorland (1995)	0.50
Chalita *et al.* (1996)	0.28
Forster *et al.* (1996) Cambridge	0.51
Forster *et al.* (1996) UKMO	0.30
Hansen *et al.* (1997b)	0.3
Berntsen *et al.* (1997) Reading	0.28
Berntsen *et al.* (1997) OsloRad	0.31
Roelofs *et al.* (1997)	0.42
van Dorland *et al.* (1997)	0.38

adjustment in the stratosphere was not taken into account. Berntsen *et al.* (1997) based their work on the Oslo 3-D CTM1 model. Two radiative forcing calculations, with two different radiative transfer models and with two different background levels for ozone, were performed. The resulting radiative forcing was estimated to be 0.28 and 0.31 Wm^{-2} for the two radiation models. Roelofs *et al.* (1997) used ozone changes predicted using the European Centre Hamburg Model version 4 (ECHAM4) coupled to a tropospheric chemistry model to compute radiative forcing. They derived a value of 0.42 Wm^{-2}.

Forster *et al.* (1996) used two different 2-D CTM models to calculate the ozone increase since preindustrial time, namely, the Cambridge and the United Kingdom Meteorological Office (UKMO) models. The calculated radiative forcing was 0.51 and 0.30 Wm^{-2}, respectively, in the two cases.

Portmann *et al.* (1997) estimated tropical tropospheric ozone from ozonesonde profiles and ozone columns derived from satellite maps. They calculated the radiative forcing to give a global contribution of 0.1-0.4 Wm^{-2} for changes in ozone since preindustrial time due to biomass burning. Clouds were not taken into account in their calculations. The largest forcing (0.4 Wm^{-2}) was calculated under the assumption that the preindustrial ozone concentration was 10 ppbv everywhere.

For radiative forcing due to tropospheric ozone changes, the uncertainties are slightly reduced since WMO (1995) and IPCC (1996). Large uncertainties remain, due to insufficient knowledge about the ozone distributions in the unperturbed as well as the present atmosphere. The ozone distribution is particularly uncertain in the tropics. Our best estimate of global-mean radiative forcing since the mid-1800s is 0.35 Wm^{-2} with an uncertainty range ±0.15 Wm^{-2}. The uncertainty range is intended to approximately bracket results from a majority of studies and is not a formal indication of uncertainty. These forcings will be compared with other sources of radiative forcing in Section 10.5.

The total radiative forcing due to ozone changes in the troposphere and the stratosphere was estimated in IPCC (1996) to be 0.3 Wm^{-2} (+0.4 Wm^{-2} due to changes in tropospheric ozone and -0.1 Wm^{-2} due to changes in stratospheric ozone). The new estimate is substantially smaller, with about 0.15 Wm^{-2} as the best-estimate radiative forcing since preindustrial times (+0.35 Wm^{-2} due to changes in tropospheric ozone and -0.20 Wm^{-2} due to changes in stratospheric ozone).

10.3.4 Indirect Forcing due to Effects of Ozone Change on Other Constituents

Bekki *et al.* (1994) have calculated the radiative forcing associated with the reduction in the methane growth rate and also the forcing associated with increased tropospheric ozone concentrations resulting from stratospheric ozone changes observed from 1979 to 1994. Their results have shown an additional negative forcing for this period of -0.03 to -0.04 Wm^{-2} (-0.02 Wm^{-2} from the CH_4 change and -0.01 to -0.02 Wm^{-2} due to tropospheric ozone changes).

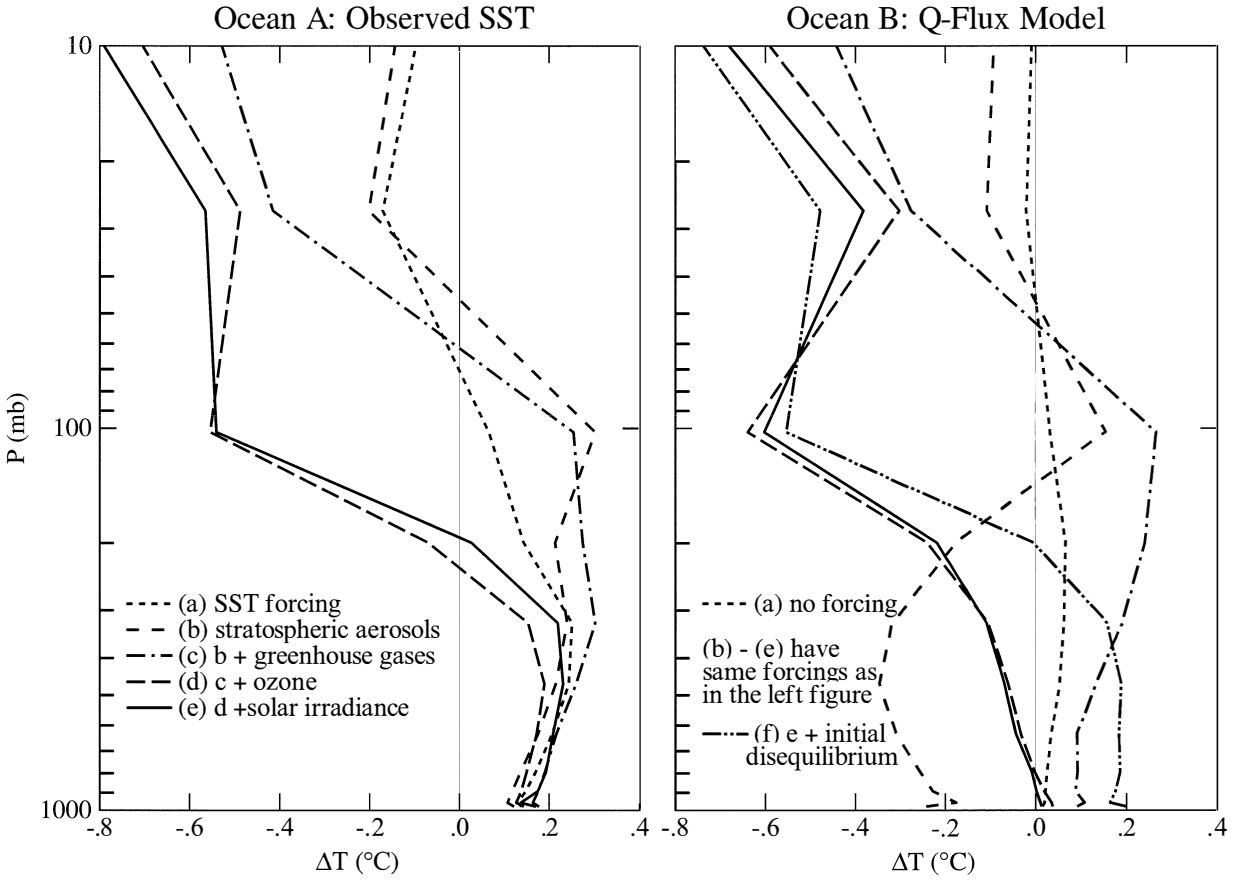

Figure 10-3. Change of the global-mean annual-mean temperature profile between 1979 and 1995 based on linear trends, calculated using the GISS GCM, as different climate forcing mechanisms are added one by one to the model. The figure on the left shows calculations using observed sea surface temperatures (SSTs). The figure on the right shows the calculation using a type of "mixed-layer" ocean model with prescribed horizontal transports of heat; on this figure the run labeled "initial disequilibrium" accounts for the fact that the climate was unlikely to be in global mean radiative balance at the top of the atmosphere at the beginning of the simulation in 1979, because of increases in greenhouse gas concentrations, and other radiative forcing mechanisms, prior to 1979. The results shown are an average of ensembles containing between five and ten members. (Figure adapted from Hansen *et al.*, 1997c.)

Another impact of stratospheric ozone depletion on climate forcing has been proposed by Toumi *et al.* (1994, 1995). OH oxidizes sulfur dioxide (SO_2) to gaseous sulfuric acid (H_2SO_4), which is a source of new H_2SO_4 particles via homogeneous nucleation; changes in the production of H_2SO_4 resulting from OH changes might affect not only the number of H_2SO_4/H_2O particles but also the number of those particles that can act as condensation nuclei. Model results suggest that OH increases resulting from ozone depletion should have increased the mean gaseous sulfuric acid production by about 2% from 1980 to 1990. This, in turn, may have increased cloud condensation nuclei (CCN) and cloud droplet numbers. Estimations of the radiative forcing related to this process give a negative radiative forcing (via increased cloud reflectivity) that might be of a magnitude similar to the direct effect of ozone loss. However, Rodhe and Crutzen (1995) disputed whether this mechanism was of importance. No further studies on this topic have been reported, to our knowledge, since the last Assessment.

10.3.5 Climate Model Studies

The climate model studies discussed in Section 10.3.2 indicate that the forcings associated with ozone change cause a significant climatic effect (see also Section 10.5). However, in terms of detecting the influence of ozone change on climate, these studies are not sufficient to explore whether the history of forcing is consistent with the magnitude of observed changes (although they can be used to look for similarities between the modeled and observed patterns of climate change (see, e.g., Santer *et al.*, 1996)).

A more realistic approach is to model the transient response of the climate system to the time-evolving forcing, and to investigate the size of the ozone effect in the context of the effect of other forcing mechanisms (both natural and due to human activity) and unforced variability. Because of the inherently chaotic nature of climate variation, the robustness of any signal can be assessed by running the model several times with slightly different initial conditions. The number of members of such ensembles is generally limited by the available computer time.

WMO (1995) reported the results from the first transient GCM experiments to investigate the climatic impact of ozone loss. Since then Tett *et al.* (1996) and Hansen *et al.* (1997c) have reported further transient studies incorporating the effects of stratospheric ozone change. We are not aware of any studies that have examined, individually, the impact of tropospheric ozone changes. Tett *et al.* (1996) used a coupled ocean-atmosphere GCM and incorporated the effects of changes in well-mixed greenhouse gases, a representation of the direct effect of sulfate aerosols, and stratospheric ozone loss for the period 1961 to 1995. Ensemble experiments, with four members, were performed with a variety of combinations of forcings, and significance was assessed using a 700-year control run of the model in which forcing was kept constant.

Hansen *et al.* (1997c) used an atmospheric GCM with a variety of representations of the ocean, ranging from fixed (observed) sea surface temperatures to a sophisticated oceanic GCM. For the period 1979 to 1996, they incorporated the forcings due to well-mixed greenhouse gases, stratospheric ozone, volcanic aerosols, and solar irradiance; the forcings were added one by one, and ensembles included between five and ten members. Control integrations, with no imposed forcing, were also performed.

In both studies, the observed cooling of the lower stratosphere, derived from radiosonde analyses, was shown to be consistent with the model when ozone loss was included; this supports earlier evidence that the stratospheric cooling is due to human activity (see Chapter 5). Another important feature of these simulations is that the transition from tropospheric warming to stratospheric cooling (which is a feature of experiments in which changes of carbon dioxide concentration are the only forcing mechanism) occurs at a significantly lower altitude when the ozone loss is incorporated. The vertical profiles of the 1979-1995 temperature trend are shown in Figure 10-3 as different forcings are added to the Hansen *et al.* (1997c) model. Results are shown for both observed sea surface temperatures and a mixed-layer ocean. The effects of ozone changes on both the transition height and on lower-stratospheric temperatures are clearly seen. When model-simulated changes in sea surface temperature are included, the transition height is even lower. The height of the transition is in much better agreement with radiosonde analyses than calculations that just include the effects of increasing well-mixed greenhouse gas concentrations.

The effect of the ozone changes on surface temperature is less clear. Both Tett *et al.* (1996) and Hansen *et al.* (1997c) (see Figure 10-3 results for Ocean B) show that the ozone loss leads to a surface cooling, as expected from the radiative forcing. In the global mean, the cooling is about 0.1°C over a 15- to 20-year period; this can be compared to a warming, due to greenhouse gas increases, of about 0.2 to 0.3°C over the same period. However, unlike the ozone effects in the upper troposphere and lower stratosphere, this change is not significant compared to natural variability and does not lead to a significant improvement in the agreement between model and observations.

Bintanja *et al.* (1997) have used their energy balance climate model to compute the transient response to ozone perturbations. Because energy balance models do not simulate unforced variability in the climate system, the impact of forcings is easily diagnosed. They used somewhat idealized ozone changes based on recent observations and calculated the transient response over a 20-year period. Changes in lower stratospheric ozone led to a surface cooling of about 0.05°C; this cooling is reduced by a factor of 2 when increases in tropospheric ozone are included. Hence, there is a significantly smaller offset of the greenhouse-gas-induced warming

in this energy balance model study than in the GCM studies. The reasons for this are not obvious; they could relate to either the form of the imposed ozone depletions or the simple type of model used.

10.4 RADIATIVE FORCINGS AND GLOBAL WARMING POTENTIALS OF HALOCARBONS

10.4.1 Introduction

This section updates work reported in WMO (1995) and IPCC (1996) on the radiative forcing and Global Warming Potentials due to the CFCs, their replacements, or proposed replacements, and related molecules. Such information is important in assessing the desirability of using particular replacements. This area is of renewed importance following the 1997 Kyoto Protocol to the United Nations (UN) Framework Convention on Climate Change; if the Protocol is ratified, reductions of greenhouse gas emissions will be calculated using a "carbon dioxide equivalence," with the (100-year) Global Warming Potentials (GWPs) forming the basis for calculating this equivalence.

10.4.2 Recent Studies on the Spectroscopy of CFCs and their Substitutes

The accurate calculation of the radiative forcing of the CFCs and related species is reliant on good-quality data on the absorption cross sections at thermal infrared wavelengths. WMO (1995) briefly reviewed earlier data. For some gases, a spread exceeding 25% of the mean cross sections was found and there was little agreement on the sign, or indeed even the existence, of any temperature dependence.

Since WMO (1995) there have been a number of studies reporting new absorption cross sections. Imasu *et al.* (1995), Heathfield *et al.* (1998a, 1998c), and Cavalli *et al.* (1998) reported measurements for a number of halogenated ethers; Barry *et al.* (1997) measured the cross sections of $CF_3CH_2CF_2CH_3$ (HFC-365mfc); Gierczak *et al.* (1996) measured the cross sections of $CF_3CH_2CF_3$ (HFC-236fa) and $CF_3CHFCHF_2$ (HFC-236ea); Christidis *et al.* (1997) reported measurements for a number of HFCs, HCFCs, bromocarbons, iodocarbons, and some ethers. Newnham and Ballard (1995), Newnham *et al.* (1996), and Smith *et al.* (1996) measured CH_2FCF_3 (HFC-134a), CH_3CClF_2 (HCFC-142b), and CH_2F_2 (HFC-32), respectively, at high spectral resolution. Wallington *et al.* (1997) and Christensen *et al.* (1998) measured $C_4F_9OCH_3$ (HFE-7100) and $C_4F_9OC_2H_5$ (HFE-7200), respectively. Molina *et al.* (1995) measured nitrogen trifluoride (NF_3). Grossman *et al.* (1997), Pappasavva *et al.* (1997), and Good *et al.* (1998) reported cross sections derived from quantum mechanical modeling and showed that these can provide a reasonable alternative to direct measurements.

The integrated band-strengths for some molecules show significant spreads. In addition to the cases highlighted in WMO (1995), recent measurements of $CHClF_2$ (HCFC-22) at, or near, room temperature range (in units of 10^{-17} cm^{-1} (molec $cm^{-2})^{-1}$) from 0.9 in McDaniel *et al.* (1991) to 0.97 in Anastasi *et al.* (1994) to 1.01 in Varanasi *et al.* (1994) and Pinnock *et al.* (1995) to 1.03 in Capellani and Restelli (1992) and Clerbaux *et al.* (1993). This gives a spread of about ±7% around the midpoint. Christidis *et al.* (1997) compiled a list of reported CCl_3F (CFC-11) cross sections; correcting for the different spectral ranges used by different investigators, they found a standard deviation of about 6% for the strongest bands.

For gases for which measurements have only recently been reported, the degree of agreement between different studies is very variable. For example, the integrated cross sections of three fluorinated ethers listed by both Imasu *et al.* (1995) and Heathfield *et al.* (1998a) agree to within 3%. Heathfield *et al.*'s value for CHF_2OCF_3 (HFE-125) is 12% higher than that given by Christidis *et al.* (1997). Cavalli *et al.*'s (1998) value for $C_4F_9OCH_3$ is about 20% higher than that reported by Wallington *et al.* (1997). For HFC-32, Smith *et al.* (1996) found a surprisingly large pressure dependence (with the integrated cross section 10% lower for air-broadening at 1000 mb than for pure vapor); for similar conditions, their integrated cross section is 20% lower than that of Pinnock *et al.* (1995) (although Pinnock *et al.*'s value is now believed to be 8% too high (M.D. Hurley, Ford Motor Company, U.S., personal communication, 1998)).

There are a number of possible reasons for the spread in values. For some species, absorption on the cell walls can occur for certain types of cells; for example R.J. Knight and J. Ballard (Rutherford Appleton Laboratory, U.K., personal communication, 1998) report initial adsorption of pure HCFC-22 onto the walls of a stainless steel cell, which reduced gas concentrations by 5-10% in 30 minutes (see also Newnham and Ballard (1995) for a discussion concerning HCFC-142b). Other

problems can occur in using gas-air mixes if it is not ensured that the mixture is sufficiently homogeneous. If uncorrected, such problems could generate errors in the integrated cross section on the order of 10%.

In conclusion, for most (but not all) gases, currently available cross sections can probably be considered to be accurate to within about 10%, but no better than 5%. To improve confidence in the measurements, the causes of the differences amongst different measurement techniques would need to be identified and, if possible, corrected.

The radiative forcing due to the CFCs and their related molecules depends also on knowledge of the spectroscopy of overlapping species such as water vapor, carbon dioxide, and ozone. A new version of the high-resolution transmission (HITRAN) molecular absorption database (Rothman *et al.*, 1992) has been released. The new version, HITRAN 1996, updates the previous version, HITRAN 1992. HITRAN includes the positions, strengths, and half-widths of the major greenhouse gases throughout the infrared spectrum. Since 1986 the number of catalogued lines in the 0-3000 cm^{-1} region has increased from about 260,000 to 870,000, but most of these are weak lines. Pinnock and Shine (1998) examined the effect of updates in the HITRAN database on calculations of radiative forcing for CO_2, CH_4, O_3, and nitrous oxide (N_2O). The effects of changes since HITRAN 1986 are less than 3%, and less than 1% since HITRAN 1992. Remaining spectroscopic uncertainties were estimated to cause errors of no more than 5% in the radiative forcing. Hence, errors from this source are likely to be smaller than current uncertainties in the absorption cross sections of the halocarbons.

10.4.3 Recent Radiative Forcing Studies

Many previous studies of the radiative forcing (which is defined in Section 10.3.2) due to CFCs and related molecules have been based on calculations with a single, normally global-mean, profile. Since the temperature, cloudiness, humidity, and ozone vary spatially, it is important to test how close the global mean of the radiative forcing is to the radiative forcing calculated with a global-mean profile.

Myhre and Stordal (1997) have considered in detail the sensitivity of the radiative forcing to both spatial and temporal averaging. For a range of well-mixed greenhouse gases, the error in the global-mean forcing was found to be about 1% or less if annual-mean rather than monthly-mean profiles were used. Similarly, the error using the daily-mean rather than the monthly-mean, or using diurnally varying rather than diurnal-mean profiles, was found to be less than 1%.

The errors due to spatial averaging were found to be more significant. Use of a single global-mean profile gave errors, for several CFCs, of around 5%. Myhre and Stordal (1997) showed that it is the latitudinal variation that must be represented to reduce this error; use of annual- and zonal-mean profiles at 10° resolution leads to an error of less than 0.5% compared to calculations at 2.5° × 2.5° resolution using monthly means. Freckleton *et al.* (1998) have shown that the error from using a global-mean profile can, for some well-mixed gases, be reduced by using just three profiles. Both Myhre and Stordal (1997) and Freckleton *et al.* (1998) have shown that alternative definitions of the position of the tropopause lead to differences in the radiative forcing of several percent.

Freckleton *et al.* (1998) examined the impact of inhomogeneities in the HFC and HCFC distributions. Distributions of five molecules, with lifetimes ranging from 2 to 26 years, were taken from a 2-D model (Wild *et al.*, 1996) assuming an idealized source distribution, predominantly in the Northern Hemisphere. The error in the global-mean forcing from assuming the gas to be well mixed at the global-mean surface concentration ranged from about 5% for gases with lifetimes exceeding 15 years, to almost 30% for gases with a two-year lifetime. Most of the error was due to vertical, rather than horizontal, inhomogeneity. The latitudinal distribution of the forcing was shown to also be affected by the averaging. The local forcing could be in error by a factor of 2 when short-lived gases were assumed to be well mixed; the sign of the error depends on the location relative to the emission sources.

IPCC (1996) reported a significant discrepancy between the radiative forcing for CFC-11 calculated using the IPCC (1990) formula (from Hansen *et al.*, 1988) and a more recent calculation (Pinnock *et al.*, 1995). Since then several other studies have investigated the CFC-11 forcing, and all conclude that the IPCC (1990) value of 0.22 $Wm^{-2}ppbv^{-1}$ is too low. Hansen *et al.* (1997a) use a GCM with an updated absorption cross section for CFC-11 (based on Christidis *et al.*, 1997) to derive their best estimate of 0.25 $Wm^{-2}ppbv^{-1}$; Myhre and Stordal (1997) also derive a value of 0.25 $Wm^{-2}ppbv^{-1}$ using their highest horizontal resolution and using a vertical profile from a chemical model. Christidis *et al.*

(1997), using their "best-guess" absorption cross section, a global-mean atmosphere, and Hansen *et al.*'s revised vertical profile, obtain 0.285 $Wm^{-2}ppbv^{-1}$. Good *et al.* (1998) obtain an instantaneous forcing of 0.25 $Wm^{-2}ppbv^{-1}$ using a global-mean atmosphere and vertical profiles from a chemical model.

On the basis of these calculations, we propose a revised value for CFC-11 of 0.25 $Wm^{-2}ppbv^{-1}$, but there remains some discrepancy amongst calculations that has not been fully resolved; sources of the discrepancy include the use of different cross sections, vertical profiles, averaging assumptions, and details of the radiation calculations.

Previous WMO and IPCC reports have reported the forcings due to CFC replacements relative to CFC-11. This procedure has clear difficulties when the CFC-11 forcing is revised, because it is unclear whether the absolute forcings for the other gases should use the original or revised CFC-11 forcing. Because of this, we present the absolute radiative forcings (in $Wm^{-2}ppbv^{-1}$), which are shown in Table 10-6. There is a need for a scaling of the literature values on the basis of whether clouds are included, whether stratospheric adjustment is performed, what atmosphere is used, and what vertical profile for the gas is assumed. The bases for these rescalings are given in the footnotes to the table, but given available information, these can only be regarded as approximate and are not always possible. It is believed that cloudy-sky, adjusted forcings are the most appropriate (see, e.g., IPCC, 1995; Hansen *et al.*, 1997a).

The number of gases for which radiative forcings are now reported has grown about threefold since previous assessments. Not all the gases in this table are likely to be used, because some will be excluded for toxicological or industrial reasons, and others are likely to be used in only small amounts in specialized applications. For completeness, however, all published values known to us are presented. Given the problems in accurate measurements of absorption cross sections and differences in methods in calculating the radiative forcing, these forcings can, at best, be regarded as accurate to 10%, and, for many, probably to no better than 20%.

Section 10.5 will present estimates of the present and possible future contributions of the replacement halocarbons to the radiative forcing.

10.4.4 Global Warming Potentials

Global Warming Potentials (GWPs) have been used in past ozone and climate assessments (WMO, 1995; IPCC, 1990, 1995, 1996) as a means of quantifying the potential integrated climate forcing of various greenhouse gases relative to carbon dioxide. GWPs have been used to motivate the choice of replacements for the CFCs and, as mentioned in Section 10.4.1, play a role in the Kyoto Protocol. In this section, after providing a brief summary of the GWP definition, we discuss and provide current estimates of both direct and indirect GWPs for numerous greenhouse gases. More details concerning the limitations of GWPs can be found in IPCC (1995, 1996).

10.4.4.1 Definitions

Knowledge of the radiative forcing of a gas (see Sections 10.3.2 and 10.4.3) is necessary in estimating the potential climate impact due to the release of some amount of that gas. However, radiative forcing does not differentiate between a gas that resides in the atmosphere for centuries and one that is destroyed in days.

AGWPs

An index that accounts for the importance of the residence time of a gas is the Absolute Global Warming Potential (AGWP) (see, e.g., IPCC, 1995). The AGWP of a species represents the integrated radiative forcing due to an instantaneous pulse of that gas over some time horizon. Mathematically, the AGWP is defined by

$$AGWP_x(t') = \int_0^{t'} F_x \exp(-t/\tau_x)dt \qquad (10\text{-}4)$$

where F_x is the radiative forcing per unit mass of species x, τ_x is the atmospheric residence time constant of species x, and t' is the time horizon of the particular AGWP calculation. Generally, F_x is defined as the radiative forcing per kilogram of the gas added to the atmosphere, leading equation (10-4) to represent the total integrated forcing due to the addition of 1 kilogram of species x at time 0 integrated to time t'. For most greenhouse gases, equation (10-4) is a simple expression with a constant radiative forcing per mass and a constant response time constant. In some cases, however, F_x will depend on the background concentration of species x or on the concentration of other gases that might absorb in similar spectral regions. In a few instances, the residence time,

τ_x, can also depend on the atmospheric composition, while in even more complicated cases, the decay of an instantaneous pulse of certain gases (notably CO_2) cannot be represented by a single decay time constant even in an unchanging atmospheric composition scenario.

GWPs

A disadvantage of the AGWP quantity is that it is generally expressed in units of $Wm^{-2}kg^{-1}yr$ or $Wm^{-2}ppmv^{-1}yr$, which is often not the most intuitive way to convey the magnitude of a species' integrated forcing. A more typically used quantity involves the comparison of the integrated forcing (AGWP) of some species to the integrated forcing of another reference gas, often chosen to be CO_2; it is normal to compare equal mass emissions of the species and reference gas. Taking CO_2 to be the reference gas, the GWP of some species x is given by

$$GWP_x(t') = \frac{\int_0^{t'} F_x \exp(-t/\tau_x)dt}{\int_0^{t'} F_{CO_2} R(t)dt} \qquad (10\text{-}5)$$

where the CO_2 forcing per unit mass, F_{CO_2}, depends on the background concentration of CO_2, and $R(t)$ represents the response function that describes the decay of an instantaneous pulse of CO_2. The GWP of a gas therefore expresses the integrated forcing of a pulse (of given small mass) of that gas relative to the integrated forcing of a pulse (of the same mass) of CO_2 over some time horizon. The GWPs of various greenhouse gases can then be easily compared to determine which will cause the greatest integrated radiative forcing over the time horizon of interest.

10.4.4.2 Direct GWPs

As discussed in IPCC (1995), atmospheric gases that absorb in infrared spectral regions generally tend to increase the net downward radiation at the tropopause because of their infrared absorptive and emissive properties. GWPs calculated considering only these forcings are referred to as *direct* GWPs because the emitted gas itself leads to additional radiative forcing. If a trace gas is present in sufficiently small quantities so that its absorption is optically thin, the radiative forcing will scale linearly with the additional atmospheric abundance of the gas. While most of the gases considered in Table 10-6 are in the optically thin limit, gases like CO_2, N_2O, and CH_4 are exceptions in which the linear scaling does not hold. The radiative forcing of each gas also depends on the concentration of species that absorb in the same spectral regions (in addition to the distribution of clouds). We assume here that the background concentrations of other gases remain constant.

The CO_2 response function used in this section is based on the "Bern" carbon cycle model (see IPCC, 1996) run for a constant mixing ratio of CO_2 over a period of 500 years; this is the same response function as used in IPCC (1996) and is a slight update on that used in WMO (1995). An analytical fit to this response function has been derived by L. Bishop (AlliedSignal Inc., U.S., personal comunication, 1998):

$$R(t) = \frac{279400 + 72240t + 730.4t^2}{279400 + 107000t + 3367t^2 + t^3} \qquad (10\text{-}6)$$

where t is the time in years. This fits the model output with an absolute error of 0.002[1].

We have also assumed a different radiative forcing per kilogram of CO_2 compared to previous assessments. In previous work (WMO, 1995; IPCC, 1995, 1996) the formula used for the radiative forcing due to a pulse of CO_2 was given by

$$\Delta F = 6.3 \ln\left(1 + \frac{\varepsilon}{C_o}\right) \qquad (10\text{-}7)$$

where C_o is the concentration of carbon dioxide before the addition of the pulse (in ppmv) and ε is the magnitude of the CO_2 pulse in (ppmv). Because this formula was intended to reproduce the results of Hansen *et al.* (1988), but did so imperfectly, we will adopt the more complicated formula directly from Hansen *et al.* (1988)

[1] The integral of the response function, which can be used in the generation of GWPs, can be derived from the analytical fit using partial fractions such that

$$\int_0^t R(s)ds = 0.89025 \ln(0.34840t + 1) + 13.872 \ln(0.034259t + 1) + 715.64 \ln(0.00029986t + 1).$$

Table 10-6. Absolute radiative forcing due to the CFCs, actual and proposed replacements, and related species. See footnotes for details of the key and scalings. Molecular weights are included to facilitate the calculation of GWPs on a mass basis.

Gas		Molecular weight	Forcing (Wm^{-2} $ppbv^{-1}$)	Notes
Chlorofluorocarbons				
CFC-11	CCl_3F	137.37	0.25	$
CFC-12	CCl_2F_2	120.91	0.32	m
CFC-13	$CClF_3$	104.46	0.25	m
CFC-113	CCl_2FCClF_2	187.38	0.30	m
CFC-114	$CClF_2CClF_2$	170.92	0.31	m
CFC-115	CF_3CClF_2	154.47	0.26	m
Hydrochlorofluorocarbons				
HCFC-21	$CHCl_2F$	102.92	0.17	c
HCFC-22	$CHClF_2$	86.47	0.22	IPCC
HCFC-123	CF_3CHCl_2	152.93	0.20	IPCC
HCFC-124	CF_3CHClF	136.48	0.22	IPCC
HCFC-141b	CH_3CCl_2F	116.95	0.14	IPCC
HCFC-142b	CH_3CClF_2	100.50	0.20	IPCC
HCFC-225ca	$CF_3CF_2CHCl_2$	202.94	0.27	IPCC
HCFC-225cb	$CClF_2CF_2CHClF$	202.94	0.32	IPCC
Hydrofluorocarbons				
HFC-23	CHF_3	70.01	0.20	IPCC
HFC-32	CH_2F_2	52.02	0.13	IPCC
HFC-41	CH_3F	34.03	0.02	pi
HFC-125	CHF_2CF_3	120.02	0.23	IPCC
HFC-134	CHF_2CHF_2	102.03	0.18	c
HFC-134a	CH_2FCF_3	102.03	0.19	IPCC
HFC-143	CHF_2CH_2F	84.04	0.13	IPCC
HFC-143a	CH_3CF_3	84.04	0.16	IPCC
HFC-152	CH_2FCH_2F	66.05	0.09	pa
HFC-152a	CH_3CHF_2	66.05	0.13	IPCC
HFC-161	CH_3CH_2F	48.06	0.03	c
HFC-227ca	$CHF_2CF_2CF_3$	170.03	0.31	c
HFC-227ea	CF_3CHFCF_3	170.03	0.30	IPCC
HFC-236cb	$CH_2FCF_2CF_3$	152.04	0.23	c
HFC-236ea	CHF_2CHFCF_3	152.04	0.30	gi
HFC-236fa	$CF_3CH_2CF_3$	152.04	0.28	mean of gi, pi
HFC-245ca	$CH_2FCF_2CHF_2$	134.05	0.23	IPCC
HFC-245cb	$CH_3CF_2CF_3$	134.05	0.26	c
HFC-272ca	$CH_3CF_2CH_3$	80.08	0.08	IPCC
HFC-365mfc	$CF_3CH_2CF_2CH_3$	148.07	0.21	b
HFC-43-10mee	$CF_3CHFCHFCF_2CF_3$	252.05	0.40	IPCC

Table 10-6, continued

Gas		Molecular weight	Forcing (Wm^{-2} $ppbv^{-1}$)	Notes
Chlorocarbons				
CH_3CCl_3		133.41	0.06	IPCC
CCl_4		153.82	0.10	IPCC
$CHCl_3$		119.38	0.02	IPCC
CH_3Cl		50.49	0.01	c, gr
CH_2Cl_2		84.93	0.03	IPCC
Bromocarbons				
CH_3Br		94.94	0.01	c, gr
CH_2Br_2		173.84	0.01	c
$CHBrF_2$		130.92	0.14	c
Halon-1211	$CBrClF_2$	165.36	0.30	c
Halon-1301	$CBrF_3$	148.91	0.32	IPCC
Iodocarbons				
CF_3I		195.91	0.23	c
CF_3CF_2I		245.92	0.26	c
Fully fluorinated species				
SF_6		146.05	0.52	m
CF_4		88.00	0.08	m
C_2F_6		138.01	0.25	m
C_3F_8		188.02	0.26	r
c-C_3F_6		150.02	0.42	pa
C_4F_{10}		238.02	0.33	r
c-C_4F_8		200.03	0.36	IPCC
C_5F_{12}		288.04	0.41	r
C_6F_{14}		338.04	0.49	r
NF_3		71.00	0.13	mo
Hydrofluoroethers and hydrochlorofluoroethers				
HFE-125	CF_3OCHF_2	136.02	0.44	mean of c, go, h
HFE-134	CHF_2OCHF_2	118.03	0.45	mean of go, h
HFE-143a	CH_3OCF_3	100.04	0.27	go
HFE-227ea	$CF_3CHFOCF_3$	186.03	0.40	i
HCFE-235da2	$CF_3CHClOCHF_2$	184.49	0.38	c
HFE-236ea2	$CF_3CHFOCHF_2$	168.04	0.44	i
HFE-236fa	$CF_3CH_2OCF_3$	168.04	0.34	i
HFE-245cb2	$CF_3CF_2OCH_3$	150.05	0.32	i
HFE-245fa1	$CHF_2CH_2OCF_3$	150.05	0.30	i
HFE-245fa2	$CF_3CH_2OCHF_2$	150.05	0.31	c
HCFE-253cb2	CH_3OCF_2CHClF	148.51	0.26	h

Table 10-6, continued

Gas		Molecular weight	Forcing (Wm^{-2} $ppbv^{-1}$)	Notes
Hydrofluoroethers and hydrochlorofluoroethers, continued				
HFE-254cb2	$CHF_2CF_2OCH_3$	132.06	0.28	i
HFE-263fb2	$CF_3CH_2OCH_3$	114.07	0.20	i
HFE-329mcc2	$CF_3CF_2OCF_2CHF_2$	236.03	0.49	i
HFE-338mcf2	$CF_3CF_2OCH_2CF_3$	218.04	0.43	i
HFE-347mcc3	$CF_3CF_2CF_2OCH_3$	200.05	0.34	i
HFE-347mcf2	$CF_3CF_2OCH_2CHF_2$	200.05	0.41	i
HFE-347mfc2	$CF_3CH_2OCF_2CHF_2$	200.05	0.47	h
HFE-356mec3	$CF_3CHFCF_2OCH_3$	182.06	0.30	i
HFE-356pcc3	$CHF_2CF_2CF_2OCH_3$	182.06	0.33	i
HFE-356pcf2	$CHF_2CF_2OCH_2CHF_2$	182.06	0.37	i
HFE-356pcf3	$CHF_2CF_2CH_2OCHF_2$	182.06	0.39	i
HFE-365mcf3	$CF_3CF_2CH_2OCH_3$	164.07	0.27	i
HFE-374pc2	$CHF_2CF_2OCH_2CH_3$	146.08	0.25	h
HFE-7100	$C_4F_9OCH_3$	250.06	0.31	w
HFE-7200	$C_4F_9OC_2H_5$	264.09	0.30	w
Other molecules				
$(CF_3)_2CF\text{-}O\text{-}CH_3$		200.05	0.31	i
$(CF_3)_2CH\text{-}O\text{-}CHF_2$		218.04	0.41	i
$(CF_3)_2CH\text{-}O\text{-}CH_3$		182.06	0.30	i
$CHF_2OCF_2OC_2F_4OCHF_2$ (H-Galden 1040x)		300.05	1.05	c
$\text{-}CF_2OCF_2\text{-}$		132.01	0.42	pa
$CH_2{=}CHCH_2OCF_2CF_2H$		158.09	0.35	h
CH_3OCH_3		46.07	0.02	go
$(CF_3)_3COH$		236.03	0.32	i
$\text{-}(CF_2)_4CH(OH)\text{-}$		230.05	0.30	i
CF_3CH_2OH		100.04	0.18	i
$CF_3CF_2CH_2OH$		150.05	0.24	i
$(CF_3)_2CHOH$		168.04	0.28	i
Fluoroamines				
$(CF_3)_2NCH_3$		167.05	0.32	i
$(CF_3)_2NCF_2CHF_2$		253.04	0.45	i
$(CF_3)_2NCH_2CF_3$		235.05	0.42	i
$(CF_3)_2NCHFCF_3$		253.04	0.42	i
$(CF_3)_2NCH_2CH_3$		181.08	0.29	i

Table 10-6, continued

Footnotes

$	See text discussion.
b	From Barry *et al.* (1997). These are cloudy-sky instantaneous forcings.
c	From Christidis *et al.* (1997). These are cloudy-sky adjusted forcings. They assume 1 ppbv of gas at all altitudes. To take account of effect of decreased concentrations in stratosphere, a simple re-scaling is performed following Freckleton *et al.* (1998). For gases whose lifetimes are less than 5 years, the forcing is multiplied by 0.8. The factors for other lifetimes are: 5 to 10 years, 0.8; 10 to 20 years, 0.9; 20-200 years, 0.95; >200 years, 1.0. (Lifetimes are listed in Tables 10-8 and 10-9.)
gi	From Gierczak *et al.* (1996). Their clear-sky instantaneous forcings have been multiplied by 0.8 to yield cloudy-sky adjusted forcings, this factor being a typical one for such gases in Pinnock *et al.* (1995) and Myhre and Stordal (1997).
go	From Good *et al.* (1998). These are cloudy-sky instantaneous forcings; their absolute forcing has been re-scaled using the revised CFC-11 absolute forcing presented here.
gr	From Grossman *et al.* (1997). These are cloudy-sky instantaneous forcings.
h	From Heathfield *et al.* (1998c). These are cloudy-sky instantaneous forcings derived using the simple method of Pinnock *et al.* (1995). Where lifetimes are available, values have been multiplied by the factors described under note c.
IPCC	Molecules whose radiative forcing is unchanged from values given in Table 2.2 of IPCC (1996) except the absolute forcing is increased by a factor of 1.14 to account for the change in the recommended forcing for CFC-11.
i	Molecules taken from Imasu *et al.* (1995). Their calculations were for a clear-sky midlatitude atmosphere. The absolute forcing used here is calculated using their forcing relative to CFC-11 and the revised CFC-11 absolute forcing presented here.
m	From Myhre and Stordal (1997). These are cloudy-sky adjusted forcings calculated on a $2.5^\circ \times 2.5^\circ$ latitude-longitude grid and then globally averaged.
mo	This is a cloudy-sky instantaneous forcing derived from information given in Molina *et al.* (1995) by K.P. Shine using the simple method given in Pinnock *et al.* (1995).
pa	From Pappasavva *et al.* (1997) who computed absorption cross sections and used the simple method of Pinnock *et al.* (1995) to derive the clear-sky instantaneous forcing. For c-C_3F_6 their value is multiplied by 1.11 (see note r); for other gases their value is used without modification.
pi	Pinnock *et al.* (1995). These are cloudy-sky adjusted forcings. To account for the decay of the gas concentration in the stratosphere, the same scheme as described under note c is used.
r	Roehl *et al.* (1995). Their absolute cloudy-sky instantaneous forcings are multiplied by 1.11 to account for stratospheric adjustment; this factor is from Myhre and Stordal (1997) for C_2F_6 and assumes all the perfluorocarbons behave like C_2F_6. The application of this factor for C_2F_6 reduces the discrepancy reported in IPCC (1996).
w	Wallington *et al.* (1997) for HFE-7100 and Christensen *et al.* (1998) for HFE-7200. These are instantaneous cloudy-sky forcings derived using the simple method of Pinnock *et al.* (1995); values have been multiplied by 0.8 to account for the short lifetime, as explained in note c.

(using the conversion factor from temperature to radiative forcing reported in IPCC (1990)):

$$\Delta F = 3.35(f(C) - f(C_o)) \qquad (10\text{-}8)$$

where

$$f(C) = \ln(1 + 1.2C + 0.005C^2 + 1.4 \times 10^{-6} C^3) \qquad (10\text{-}9)$$

We assume a background CO_2 concentration of 364 ppmv, close to the present-day value (WMO (1995) used 354 ppmv). For this assumption, this expression agrees well with the adjusted cloudy-sky radiative forcing calculations of Myhre and Stordal (1997); see also Myhre *et al.* (1998b). The revised forcing is about 12% lower than that derived using the original IPCC expression. For a small perturbation in CO_2 from 364 ppmv, the forcing is 0.01548 $Wm^{-2}ppmv^{-1}$. This value is used in the GWP calculations presented here. Because of the changes in the CO_2 response function from WMO (1995) and the changes in the CO_2 forcing per mass, the CO_2 AGWPs differ from the values used in WMO (1995) by -12%, -9%, and -9% for the 20-, 100-, and 500-year time horizons, respectively. These decreases in the CO_2 AGWPs will lead to slightly larger GWPs for other gases, in the absence of other changes. The CO_2 AGWPs assumed for this chapter and those assumed in WMO (1995) are shown in Table 10-7. In order to allow traceability between different tabulations of GWPs, Table 10-7 also shows the AGWPs using the CO_2 decay function used in WMO (1995) and IPCC (1995) and the revised CO_2 forcing, and the new decay function and the original forcing.

In Tables 10-8 and 10-9, the direct GWPs (on a mass basis) for 88 gases are tabulated for time horizons of 20, 100, and 500 years in order to illustrate the radiative forcing impact over various integration times. The list consists of CFCs, HCFCs, HFCs, hydrochlorocarbons, bromocarbons, iodocarbons, fully fluorinated species, fluoroalcohols, and fluoroethers. The radiative forcings per kilogram were derived from the values given per ppbv in Table 10-6.

The lifetimes come from a variety of sources. Where revised recommendations have been made in Chapters 1 and 2, their values are adopted. For most of the other gases, the values given in Table 2.2 of IPCC (1996) are used; these values do not take into account the slight revision in methyl chloroform lifetime discussed in Chapter 2. Exceptions are CH_3CF_3 (HFC-143a) (+11%) and HFC-236fa (+8%); their increased lifetimes result from revised rate constants for reaction with OH (De More *et al.*, 1997) (and have been scaled to the revised OH lifetime for methyl chloroform given in Chapter 2). For species not previously listed, lifetimes have been taken from Imasu *et al.* (1995), Christensen *et al.* (1998), Christidis *et al.* (1997), Gierczak *et al.* (1996), Good *et al.* (1998), Heathfield *et al.* (1998b),

Table 10-7. Absolute Global Warming Potentials for carbon dioxide for time horizons of 20, 100, and 500 years. The value for the previous Assessment (WMO, 1995) is also shown, as well as the impact, individually, of the changes in the CO_2 forcing and the response function. Note that the WMO (1995) values are as used in IPCC (1995). The IPCC (1996) report used the revised response function but the old forcing; hence the absolute GWPs used in IPCC (1996) are those shown in the final row of this table.

	Absolute Global Warming Potentials (Wm^{-2} yr $ppmv^{-1}$)		
	20-Year	**100-Year**	**500-Year**
This work	0.207	0.696	2.241
WMO (1995)	0.235	0.768	2.459
Using the revised forcing but the WMO (1995) response function	0.209	0.684	2.188
Using the WMO (1995) forcing but the revised response function	0.238	0.800	2.576

Table 10-8. Direct Global Warming Potentials (mass basis) relative to carbon dioxide (for gases for which the lifetimes have been adequately characterized).

Gas		Lifetime (years)	Global Warming Potential (Time Horizon in years)		
			20 years	100 years	500 years
Carbon dioxide	CO_2	See text	1	1	1
Methane[1]	CH_4	12.2* (a)	64	24	7.5
Nitrous oxide[2]	N_2O	120 (b)	330	360	190
Chlorofluorocarbons					
CFC-11	CCl_3F	45 (b)	6300	4600	1600
CFC-12	CCl_2F_2	100 (b)	10200	10600	5200
CFC-13	$CClF_3$	640 (c)	10000	14000	16300
CFC-113	CCl_2FCClF_2	85 (b)	6100	6000	2700
CFC-114	$CClF_2CClF_2$	300 (a)	7500	9800	8700
CFC-115	CF_3CClF_2	1700 (a)	7100	10300	14300
Hydrochlorofluorocarbons					
HCFC-21	$CHCl_2F$	2.0 (d)	700	210	65
HCFC-22	$CHClF_2$	11.8 (b)	5200	1900	590
HCFC-123	CF_3CHCl_2	1.4 (a)	390	120	36
HCFC-124	CF_3CHClF	6.1 (a)	2000	620	190
HCFC-141b	CH_3CCl_2F	9.2 (b)	2100	700	220
HCFC-142b	CH_3CClF_2	18.5 (b)	5200	2300	720
HCFC-225ca	$CF_3CF_2CHCl_2$	2.1 (a)	590	180	55
HCFC-225cb	$CClF_2CF_2CHClF$	6.2 (a)	2000	620	190
Hydrofluorocarbons					
HFC-23	CHF_3	243 (b)	11700	14800	11900
HFC-32	CH_2F_2	5.6 (a)	2900	880	270
HFC-41	CH_3F	3.7 (a)	460	140	43
HFC-125	CHF_2CF_3	32.6 (a)	6100	3800	1200
HFC-134	CHF_2CHF_2	10.6 (a)	3400	1200	370
HFC-134a	CH_2FCF_3	13.6 (b)	4100	1600	500
HFC-143	CHF_2CH_2F	3.8 (a)	1200	370	120
HFC-143a	CF_3CH_3	53.5 (d)	6800	5400	2000
HFC-152	CH_2FCH_2F	0.5 (d)	140	43	13
HFC-152a	CH_3CHF_2	1.5 (a)	630	190	58
HFC-161	CH_3CH_2F	0.25 (i)	33	10	3
HFC-227ea	CF_3CHFCF_3	36.5 (a)	5800	3800	1300
HFC-236cb	$CH_2FCF_2CF_3$	14.6 (i)	3500	1400	430
HFC-236ea	CHF_2CHFCF_3	8.1 (j)	3100	1000	310
HFC-236fa	$CF_3CH_2CF_3$	226 (d)	7500	9400	7300
HFC-245ca	$CH_2FCF_2CHF_2$	6.6 (a)	2300	720	220
HFC-365mfc	$CF_3CH_2CF_2CH_3$	10.2 (k)	2600	910	280
HFC-43-10mee	$CF_3CHFCHFCF_2CF_3$	17.1 (a)	4000	1700	530

Table 10-8, continued

Gas		Lifetime (years)	Global Warming Potential (Time Horizon in years)		
			20 years	100 years	500 years
Chlorocarbons					
CH_3CCl_3		4.8 (b)	450	140	42
CCl_4		35 (b)	2100	1400	450
$CHCl_3$		0.51 (a)	18	5	2
CH_3Cl		1.3 (b)	55	16	5
CH_2Cl_2		0.46 (a)	35	10	3
Bromocarbons					
CH_3Br		0.7 (b)	16	5	1
CH_2Br_2		0.41 (i)	5	1	<1
$CHBrF_2$		7.0 (i)	1500	470	150
Halon-1211	$CBrClF_2$	11 (b)	3600	1300	390
Halon-1301	$CBrF_3$	65 (b)	7900	6900	2700
Iodocarbons					
CF_3I		0.005 (a)	1	<1	<<1
Fully fluorinated species					
SF_6		3200 (a)	15100	22200	32400
CF_4		50000 (a)	3900	5700	8900
C_2F_6		10000 (a)	7700	11400	17300
C_3F_8		2600 (a)	5900	8600	12400
C_4F_{10}		2600 (a)	5900	8600	12400
c-C_4F_8		3200 (a)	7600	11200	16400
C_5F_{12}		4100 (a)	6000	8900	13200
C_6F_{14}		3200 (a)	6100	9000	13200
Ethers and Halogenated Ethers					
CH_3OCH_3		0.015 (e)	1	<1	<<1
HFE-125	CF_3OCHF_2	165 (e)	13000	15300	10000
HFE-134	CHF_2OCHF_2	29.7 (e)	11800	6900	2200
HFE-143a	CH_3OCF_3	5.7 (e)	3200	970	300
HCFE-235da2	$CF_3CHClOCHF_2$	2.6 (i)	1100	340	110
HFE-245fa2	$CF_3CH_2OCHF_2$	4.4 (i)	1900	570	180
HFE-254cb2	$CHF_2CF_2OCH_3$	0.22 (h)	86	25	8
HFE-7100	$C_4F_9OCH_3$	5.0 (f)	1300	390	120
HFE-7200	$C_4F_9OC_2H_5$	0.77 (g)	190	55	17

Table 10-8, continued

Footnotes

1 The methane GWPs include an indirect contribution from stratospheric H_2O and O_3 production; the values are taken from IPCC (1996) and re-scaled to the revised AGWP for CO_2.
2 The nitrous oxide GWPs are taken from IPCC (1996) and re-scaled to the revised AGWP for CO_2.
* This value for methane is the "adjustment time," which incorporates the effect of an emission of methane on its own lifetime (see IPCC, 1995, 1996); the value used here is taken from IPCC (1996).
(a) Taken from IPCC (1996).
(b) Taken from Chapters 1 and 2 of this report.
(c) Taken from WMO (1995).
(d) Derived by J.S. Daniel using OH reaction rates at 277 K from De More *et al.* (1997), scaling to an OH lifetime for CH_3CCl_3 of 5.7 years (see Chapter 2).
(e) Good *et al.* (1998).
(f) Wallington *et al.* (1997).
(g) Christensen *et al.* (1998).
(h) Heathfield *et al.* (1998b).
(i) Taken from Christidis *et al.* (1997).
(j) Gierczak *et al.* (1996).
(k) Barry *et al.* (1997).

Molina *et al.* (1995), and Wallington *et al*. (1997). For $CHCl_2F$ (HCFC-21) and CH_2FCH_2F (HFC-152) the lifetime was calculated from the rate constant for reaction with OH (from De More *et al.*, 1997) scaled to the rate constant for the reaction of CH_3CCl_3 and OH at 277 K (following the method of Prather and Spivakovsky (1990)), using the revised methyl chloroform lifetime from Chapter 2; it is assumed that reaction with OH is the dominant loss mechanism. For many of the fluoroethers, lifetimes have not been derived from laboratory measurements of the reaction rate with OH, but have been estimated by various other means. For this reason, the lifetimes, and hence the GWPs, are considered to be much less reliable, and so these gases are listed separately in Table 10-9. NF_3 is also listed in Table 10-9, because, although its photolytic destruction has been characterized, other loss processes may be significant but have not yet been characterized (Molina *et al.*, 1995). Note also that some gases, for example, trifluoromethyl iodide (CF_3I) and dimethyl ether (CH_3OCH_3) have very short lifetimes (less than a few months); GWPs for such short-lived gases need to be treated with caution, because the gases are unlikely to be evenly distributed globally, and hence estimates of, for example, their radiative forcing using global-mean conditions, may be subject to error.

Uncertainties in the lifetimes of CFC-11 and CH_3CCl_3 are thought to be about 10%, while uncertainties in the lifetimes of gases obtained relative to CFC-11 or CH_3CCl_3 are somewhat larger (20-30%) (WMO, 1995). Uncertainties in the radiative forcing per mass of the majority of the gases considered in Table 10-6 are approximately ±10%. IPCC (1996) suggested typical uncertainties of ±35% for the GWPs, and we retain this uncertainty estimate for gases listed in Table 10-8. In addition to uncertainties in the CO_2 forcing per kilogram and in the response function, AGWPs of CO_2 are affected by assumptions concerning future CO_2 abundances. Saturation of absorption features at various wavelengths causes the radiative forcing due to a pulse of CO_2 to depend on the assumed background concentrations of CO_2. Furthermore, as the background CO_2 concentrations change, the pulse response function changes as well. In spite of these dependencies on the choice of a future CO_2 scenario, it remains likely that the error introduced by these assumptions is smaller than the uncertainties introduced by our imperfect understanding of the carbon cycle (WMO, 1995; IPCC, 1996). Finally, although any induced error in the CO_2 AGWPs will certainly affect the non-CO_2 GWPs, it will not affect intercomparisons among non-CO_2 GWPs.

Table 10-9. Direct Global Warming Potentials (mass basis) relative to carbon dioxide (for gases for which the lifetime has been determined only via indirect means, rather than laboratory measurements, or for which there is uncertainty over the loss processes).

Gas		Lifetime (years)	Global Warming Potential (Time Horizon in years)		
			20	100	500
NF_3		740 (a)	7700	10800	13100
HFE-227ea	$CF_3CHFOCF_3$	11 (b)	4200	1500	460
HFE-236ea1	$CF_3CHFOCHF_2$	5.8 (b)	3100	960	300
HFE-236fa	$CF_3CH_2OCF_3$	3.7 (b)	1600	470	150
HFE-245cb2	$CF_3CF_2OCH_3$	1.2 (b)	540	160	50
HFE-245fa1	$CHF_2CH_2OCF_3$	2.2 (b)	940	280	86
HFE-263fb2	$CF_3CH_2OCH_3$	0.1 (b)	37	11	3
HFE-329mcc2	$CF_3CF_2OCF_2CHF_2$	6.8 (b)	2800	890	280
HFE-338mcf2	$CF_3CF_2OCH_2CF_3$	4.3 (b)	1800	540	170
HFE-347mcc3	$CF_3CF_2CF_2OCH_3$	1.3 (b)	470	140	43
HFE-347mcf2	$CF_3CF_2OCH_2CHF_2$	2.8 (b)	1200	360	110
HFE-356mec3	$CF_3CHFCF_2OCH_3$	0.94 (b)	330	98	30
HFE-356pcc3	$CHF_2CF_2CF_2OCH_3$	0.93 (b)	360	110	33
HFE-356pcf2	$CHF_2CF_2OCH_2CHF_2$	2.0 (b)	860	260	80
HFE-356pcf3	$CHF_2CF_2CH_2OCHF_2$	1.3 (b)	590	180	55
HFE-365mcf3	$CF_3CF_2CH_2OCH_3$	0.11 (b)	38	11	4
HFE-374pc2	$CHF_2CF_2OCH_2CH_3$	0.43 (b)	160	47	14
$(CF_3)_2CFOCH_3$		3.5 (b)	1100	340	110
$(CF_3)_2CHOCHF_2$		3.1 (b)	1200	370	110
$(CF_3)_2CHOCH_3$		0.25 (b)	88	26	8
$CHF_2OCF_2OC_2F_4OCHF_2$ (H-Galden 1040x)		48 (c)	12200	9300	3300
$-(CF_2)_4CH(OH)-$		0.85 (b)	240	70	22
CF_3CH_2OH		0.46 (b)	180	52	16
$CF_3CF_2CH_2OH$		0.43 (b)	150	43	14
$(CF_3)_2CHOH$		1.4 (b)	500	150	46

(a) Molina *et al*. (1995).
(b) Imasu *et al*. (1995).
(c) Christidis *et al*. (1997).

10.4.4.3 Indirect GWPs

Some trace species can exert a radiative forcing by their involvement in chemical reactions that alter the concentrations of other radiatively active gases. This forcing is referred to as an "indirect" forcing because the radiative change is caused by another species that is chemically perturbed by the presence of the trace gas, and not by absorption and emission of radiation by the trace gas itself. While direct GWPs are usually believed to be known reasonably accurately (±35%), indirect GWPs can be highly uncertain.

Methane

Four types of indirect effects due to the presence of atmospheric methane have been identified. The largest effect is potentially the production of ozone. This effect is difficult to quantify, however, because the magnitude of ozone production is highly dependent on the abundance and distribution of NO_x (IPCC, 1996). Other indirect effects include the production of stratospheric water vapor, the production of carbon dioxide (from certain methane sources), and the increase in the methane adjustment time resulting from its coupling with OH (Brühl, 1993; Lelieveld and Crutzen, 1992; Prather, 1994, 1996; IPCC 1996). Because no additional calculations of the CH_4 GWPs have been presented since IPCC (1996), we adopt their values with a correction for our different CO_2 AGWPs. It should be noted that the climate forcing caused by CO_2 produced from the oxidation of CH_4 is not included in these GWP estimates. As discussed in IPCC (1996), it is often the case that this CO_2 is included in national carbon production inventories. Therefore, depending on how the inventories are combined, including the CO_2 production from CH_4 could result in "double counting" the radiative forcing of this CO_2.

Carbon Monoxide

Carbon monoxide leads to indirect radiative effects that are similar to those of methane. Unlike methane, however, the direct radiative forcing is likely to be significantly smaller than its indirect forcing (Evans and Puckrin, 1995; Sinha and Toumi, 1996; Daniel and Solomon, 1998). An atmospheric pulse of CO can lead to the production of ozone, with the magnitude of ozone formation dependent on the amount of NO_x present. As with methane, this effect is quite difficult to quantify due to the highly variable and uncertain NO_x distribution (Emmons *et al.*, 1997). The emission of CO also perturbs OH, which can then lead to an increase in the CH_4 concentration (Prather, 1996; Daniel and Solomon, 1998). Finally, the oxidation of the CO from fossil fuel emission by reaction with OH results in the formation of CO_2. Because of the difficulty in accurately calculating the amount of ozone produced by the addition of a pulse of CO, an accurate estimate of the entire indirect forcing of CO would most likely require a 3-D model. Because of the difficulties in calculating a CO GWP, we mention here only that Daniel and Solomon (1998), using a box model, have estimated an upper limit of 4 for the CO indirect GWP for the 100-year time horizon; it is likely that the actual value is closer to their lower limit of 1. As with CH_4, the production of CO_2 from oxidized CO can lead to double counting of this CO_2 and is therefore not considered in these estimates.

Halocarbons

In addition to their direct radiative forcing, chlorinated and brominated halocarbons can lead to a significant indirect forcing through their destruction of stratospheric ozone. By destroying stratospheric ozone, itself a greenhouse gas, halocarbons are likely to induce a negative indirect forcing that counteracts some or perhaps all, in certain cases, of their direct forcing. Quantifying the magnitude of the negative indirect forcing is quite difficult for several reasons. As discussed in Section 10.3, the negative forcing arising from the ozone destruction is highly dependent on the altitude profile of the ozone loss. Furthermore, the additional radiative effects due to enhanced tropospheric OH are potentially important and similarly difficult to quantify (Section 10.3.4). While recognizing these uncertainties, estimates have been made of the net radiative forcing due to particular halocarbons, which can then be used to determine net GWPs (including both direct and indirect effects). This was done by Daniel *et al.* (1995), where it was shown that if the enhanced tropospheric OH effect were ignored, and the negative forcing due to ozone loss during the 1980s was -0.08 Wm^{-2}, the net GWPs for the bromocarbons were significantly negative, illustrating the impact of the negative forcing arising from the bromocarbon-induced ozone depletion. While the effect on the chlorocarbon GWPs was less pronounced, it was significant as well. In Table 10-10 we have updated the indirect GWP results from Daniel *et al.* (constant-alpha case A) (but with the alpha increased from 40 to 60; see Chapter 2) to reflect the updated forcing and response of CO_2 and to account for an uncertainty in the 1980-1990

Table 10-10. Net Global Warming Potentials (mass basis) of selected halocarbons. (Updated from Daniel *et al.*, 1995.)

Species	Time Horizon = 2010 (20 years)			Time Horizon = 2090 (100 years)		
	Direct	Min	Max	Direct	Min	Max
CFC-11	6200	-840	5090	4600	-1680	3610
CFC-12	10200	6720	9650	10600	6900	10020
CFC-113	6100	1970	5450	6000	1740	5330
CH_3CCl_3	450	-2370	0	140	-750	0
CCl_4	2100	-6530	740	1400	-5850	260
HCFC-22	5200	4330	5060	1900	1500	1840
HCFC-123	390	-90	310	120	0	100
HCFC-124	2000	1510	1920	620	450	590
HCFC-141b	2100	-70	1760	700	-130	570
HCFC-142b	5200	4300	5060	2300	1740	2210
Halon-1301	7900	-99850	-9110	6900	-97030	-9510

ozone radiative forcing of -0.03 to -0.19 Wm^{-2}. If the Daniel *et al.* analysis had considered the OH indirect effects, the GWPs in Table 10-10 would be further reduced.

10.5 PERSPECTIVE: THE NET EFFECT OF OZONE AND HALOCARBON CHANGES AND COMPARISONS WITH OTHER FORCINGS

As has been discussed in, for example, IPCC (1995, 1996) and Hansen *et al.* (1997c), there are a large number of ways in which human activity may affect radiative forcing. In addition to the effects of the well-mixed greenhouse gases and ozone, changes in aerosol concentrations resulting from fossil-fuel and biomass burning and changes in land use can all cause a radiative forcing both directly, by altering the scattering and absorbing properties of the atmosphere, and indirectly, via changes in cloud properties. Changes in solar irradiance and explosive volcanic eruptions also contribute.

The global-mean forcing due to well-mixed greenhouse gases is about 2.25 to 2.5 Wm^{-2} since preindustrial times (e.g., IPCC, 1996; Myhre *et al.*, 1998b). Although this is several times the forcing due to ozone change, the ozone effects are significant. Changes in tropospheric ozone may enhance this forcing by 10 to 15% and, at the upper end of its uncertainty range, it may be of similar importance to methane, which is the second most important contributor to the well-mixed greenhouse gas forcing (with about 0.5 Wm^{-2} since preindustrial times).

In addition, the tropospheric ozone forcing is of a similar size, but opposite sign, to many recent estimates of the direct forcing due to sulfate aerosols (see, e.g., IPCC 1996; van Dorland *et al.*, 1997; Feichter *et al.*, 1997; Chuang *et al.*, 1997). (The indirect forcing due to the impact of increased aerosols on cloud properties is highly uncertain but may be as negative as -1.5 Wm^{-2} (e.g., IPCC, 1996; Feichter *et al.*, 1997; Chuang *et al.*, 1997).) The direct effect of sulfate aerosols has been included in several studies that have attempted to attribute climate changes to human activity (e.g., Santer *et al.*, 1996; Tett *et al.*, 1996; Mitchell *et al.*, 1995; Haywood *et al.*, 1997) whereas tropospheric ozone has not. Further, black carbon from fossil fuel and biomass burning may cause a significant positive forcing of a similar size (at least on a global-mean basis) but opposite sign to the sulfate aerosol effect (e.g., IPCC, 1996; Haywood and Ramaswamy, 1998; Hansen *et al.*, 1997c), and other components of the aerosol population may be significant (see, e.g., Tegen *et al.*, 1997). The direct effect of all aerosols may be much smaller than the effect of sulfate alone. Hence, the inclusion of changes in tropospheric ozone seems likely to be as important as the direct effect

of aerosols in studies attempting to detect and attribute the effect of human activity on climate.

The radiative forcing due to stratospheric ozone change is of a similar magnitude but opposite sign to the tropospheric ozone forcing. While it is important at the 10% level compared to the well-mixed greenhouse gas forcing since preindustrial times, as has been pointed out in earlier assessments, its importance over the shorter term may be considerably greater, given that most of its effect has occurred over the two most recent decades. The forcing since the late 1970s due to the well-mixed greenhouse gases is about 0.5 Wm^{-2}, so the ozone loss may have offset about 30% of this forcing. The ozone forcing constitutes an even higher proportion of the forcing due to the halocarbons that lead to the ozone loss. The total direct forcing from the halocarbons is about 0.25 Wm^{-2} (see, e.g., IPCC, 1996), so our midrange estimate of the stratospheric ozone forcing offsets about 80% of this.

With the exception of HCFC-22, all the halogenated replacements are currently present in concentrations of only pptv, or less, so their contribution to radiative forcing is currently negligible. Using the global-mean concentrations from Chapter 2 and the forcings per ppbv from Table 10-6, the forcing due to HCFC-22 is about 0.025 Wm^{-2} (IPCC, 1996), which is about an order of magnitude lower than the current contributions from all the CFCs. The total contribution using the 1996 concentrations of CH_3CClF_2 (HCFC-142b), CH_3CCl_2F (HCFC-141b), and HFC-134a, from Chapter 2, gives a forcing of just a few thousandths of a Watt per square meter. Similarly the contributions from sulfur hexafluoride (SF_6) and the perfluorocarbons, using concentrations from Chapter 1, sum to less than 0.01 Wm^{-2}. The contribution from perfluoromethane (CF_4) is reduced from that given in IPCC (1996) because it was assumed there that the preindustrial concentration was zero whereas, as discussed in Chapter 1, there is evidence that the preindustrial concentration was 40 pptv (compared to a present-day concentration of about 70 pptv).

As reported in Chapters 1 and 2, the growth rate for many of the replacement species is high and their contribution to the rate of change of forcing is somewhat higher than their contribution to the cumulative forcing. For example, for SF_6, the forcing is about 0.1% of the forcing due to CO_2 since preindustrial times, but its current rate of change of forcing is 0.4% of the current rate of change of forcing due to CO_2. The values for CHF_3 (HFC-23) and CF_4 are similar.

Looking into the future, based on the estimates of the greenhouse gas concentrations in the 21st century from IPCC Scenario IS92a, as reported in IPCC (1996), the contribution of the HFCs would rise to 0.23 Wm^{-2} by the year 2100, which can be compared to a total forcing from greenhouse gases, using the same scenario, of about 6 Wm^{-2}. These scenarios are, of course, highly uncertain given the nature of many of the underlying assumptions. The contributions due to the HCFCs after reaching a peak, at about double current levels, in around 2005, are expected to fall to zero by 2100, as a result of their phaseout under the terms of the Montreal Protocol and its Amendments. The contribution of CFCs is expected to fall to less than 0.1 Wm^{-2} by 2100.

In conclusion, changes in ozone are an important contributor to the overall radiative forcing picture, and refinement of our understanding of these forcings will be important if our understanding of the wider impact of human activity on the climate is to be understood. Although stratospheric ozone depletion has partly offset the effects of any greenhouse-gas-induced forcing over the past decade, it may not continue to do so. If ozone recovers as is anticipated (see Chapter 12), the decadal increase in forcing due to the ozone recovery may, in the early part of the next century, enhance, by about 10%, the decadal increase in forcing due to the other greenhouse gases (Solomon and Daniel, 1996).

REFERENCES

Anastasi, C., A.E. Heathfield, G.P. Knight, and F. Nicolaisen, Integrated absorption-coefficients of $CHClF_2$ (HCFC-22) and CH_3Br in the atmospheric infrared window region, *Spectrochim. Acta*, *50A*, 1791-1798, 1994.

Anklin, M., and R.C. Bales, Recent increase in H_2O_2 concentration at Summit, Greenland, *J. Geophys. Res.*, *102*, 19099-19104, 1997.

Barry, J., G. Locke, D. Scollard, H. Sidebottom, J. Treacy, C. Clerbaux, R. Colin, and J. Franklin, 1,1,1,3,3,-pentafluorobutane (HFC-365mfc): Atmospheric degradation and contribution to radiative forcing, *Int. J. Chem. Kinet.*, *29*, 607-617, 1997.

Bekki, S., K.S. Law, and J.A. Pyle, Effect of ozone depletion on atmospheric CH_4 and CO concentrations, *Nature*, *371*, 595-597, 1994.

Berntsen, T., I.S.A. Isaksen, J.S. Fuglestvedt, G. Myhre, F. Stordal, R.S. Freckleton, and K.P. Shine, Effects of anthropogenic emissions on tropospheric ozone and radiative forcing, *J. Geophys. Res.*, *102*, 28101-28126, 1997.

Bintanja, R., J.P.F. Fortuin, and H. Kelder, Simulation of the meridionally and seasonally varying climate response caused by changes in ozone concentration, *J. Clim.*, *10*, 1288-1311, 1997.

Brühl, C., The impact of the future scenarios for methane and other chemically active gases on the GWP of methane, *Chemosphere*, *26*, 731-738, 1993.

Capellani, F., and G. Restelli, Infrared band strengths and their temperature dependence of the hydrohalocarbons HFC-134a, HFC-152a, HCFC-22, HCFC-123, and HCFC-142b, *Spectrochim. Acta*, *48A*, 1127-1131, 1992.

Cavalli, F., M. Glasius, J. Hjorth, B. Rindone, and N.R. Jensen, Atmospheric lifetimes, infrared spectra and degradation products of a series of hydrofluoroethers, *Atmos. Environ.*, *32*, 3767-3773, 1998.

Chalita, S., D.A. Hauglustaine, H. Le Treut, and J.-F. Müller, Radiative forcing due to increased tropospheric ozone concentrations, *Atmos. Environ.*, *30*, 1641-1646, 1996.

Christensen, L.K., J. Sehested, O.J. Nielsen, M. Bilde, T.J. Wallington, A. Guschin, L.T. Molina, and M.J. Molina, Atmospheric chemistry of HFE-7200 ($C_4F_9OC_2H_5$): Reaction with OH radicals, fate of $C_4F_9OCH_2CH_2O\cdot$ and $C_4F_9OCHO\cdot CH_3$ radicals, *J. Phys. Chem. A*, *102*, 4839-4845, 1998.

Christidis, N., M.D. Hurley, S. Pinnock, K.P. Shine, and T.J. Wallington, Radiative forcing of climate change by CFC-11 and possible CFC replacements, *J. Geophys. Res.*, *102*, 19597-19609, 1997.

Chuang, C.C., J.E. Penner, K.E. Taylor, A.S. Grossman, and J.J. Walton, An assessment of the radiative effects of anthropogenic sulfate, *J. Geophys. Res.*, *102*, 3761-3778, 1997.

Clerbaux, C., R. Colin, P.C. Simon, and C. Granier, Infrared cross sections and global warming potentials of 10 alternative hydrohalocarbons, *J. Geophys. Res.*, *98*, 10491-10497, 1993.

Cox, S.J., W.-C. Wang, and S.E. Schwartz, Climate response to radiative forcings by sulfate aerosols and greenhouse gases, *Geophys. Res. Lett*, *22*, 2509-2512, 1995.

Crutzen, P., Global tropospheric chemistry, in *Low Temperature Chemistry of the Atmosphere*, edited by G.K. Moortgat *et al.*, pp. 465-498, Springer-Verlag, Berlin, 1994.

Daniel, J.S., and S. Solomon, On the climate forcing of carbon monoxide, *J. Geophys. Res.*, *103*, 13249-13260, 1998.

Daniel, J.S., S. Solomon, and D. Albritton, On the evaluation of halocarbon radiative forcing and global warming potentials, *J. Geophys. Res.*, *100*, 1271-1285, 1995.

DeMore, W.B, S.P. Sander, D.M. Golden, R.F. Hampson, M.J. Kurylo, C.J. Howard, A.R. Ravishankara, C.E. Kolb, and M.J. Molina, *Chemical Kinetics and Photochemical Data for Use in Stratospheric Modeling*, *Evaluation Number 11*, JPL Publ. 94-26, Jet Propulsion Laboratory, Pasadena, Calif., 1994.

DeMore, W.B., S.P. Sander, D.M. Golden, R.F. Hampson, M.J. Kurylo, C.J. Howard, A.R. Ravishankara, C.E. Kolb, and M.J. Molina, *Chemical Kinetics and Photochemical Data for Use in Stratospheric Modeling*, *Evaluation Number 12*, JPL Publ. 97-4, Jet Propulsion Laboratory, Pasadena, Calif., 1997.

Dlugokencky, E.J., K.A. Masarie, P.M. Lang, P.P. Tans, L.P. Steele, and E.G. Nisbet, A dramatic decrease in the growth rate of atmospheric methane in the Northern Hemisphere during 1992, *Geophys. Res. Lett.*, *21*, 45-48, 1994.

Emmons, L.K., M.A. Carroll, D.A. Hauglustaine, G.P. Brasseur, C. Atherton, J. Penner, S. Sillman, H. Levy, F. Rohrer, W.M.F. Wauben, P.F.J. VanVelthoven, Y. Wang, D. Jacob, P. Bakwin, R. Dickerson, B. Doddridge, C. Gerbig, R. Honrath, G. Hübler, D. Jaffe, Y. Kondo, J.W. Munger, A. Torres, and A. Volz-Thomas, Climatologies of NO_x and NO_y: A comparison of data and models, *Atmos. Environ.*, *31*, 1851-1904, 1997.

Evans, W.F.J., and E. Puckrin, An observation of the greenhouse radiation associated with carbon monoxide, *Geophys. Res. Lett.*, *22*, 925-928, 1995.

Feichter, J., U. Lohmann, and I. Schult, The atmospheric sulfur cycle in ECHAM-4 and its impact on the shortwave radiation, *Clim. Dyn.*, *13*, 235-246, 1997.

Fishman, J., The global consequences of increasing tropospheric ozone concentrations, *Chemosphere*, *22*, 685-695, 1991.

Forster, P.M. de F., and K.P. Shine, Radiative forcing and temperature trends from stratospheric ozone changes, *J. Geophys. Res.*, *102*, 10841-10857, 1997.

Forster, P.M. de F., C.E. Johnson, K.S. Law, J.A. Pyle, and K.P. Shine, Further estimates of radiative forcing due to tropospheric ozone changes, *Geophys. Res. Lett.*, *23*, 3321-3324, 1996.

Forster, P.M. de F., R.S. Freckleton, and K.P. Shine, On aspects of the concept of radiative forcing, *Clim. Dyn.*, *13*, 547-560, 1997.

Freckleton, R.S., E.J. Highwood, K.P. Shine, O. Wild, K.S. Law, and M.G. Sanderson, Greenhouse gas radiative forcing: Effects of averaging and inhomogeneities in trace gas distribution, *Quart. J. Roy. Meteorol. Soc.*, *124*, 2099-2127, 1998.

Fuglestvedt, J.S., J.E. Jonson, and I.S.A. Isaksen, Effects of reductions in stratospheric ozone on tropospheric chemistry through changes in photolysis rates, *Tellus*, *46B*, 172-192, 1994.

Fuglestvedt, J.S., J.E. Jonson, W.-C. Wang, and I.S.A. Isaksen, Response in tropospheric chemistry to changes in UV fluxes, temperatures and water vapor densities, in *Atmospheric Ozone as a Climate Gas*, edited by W.-C. Wang and I.S.A. Isaksen, NATO Series I 32, 143-162, Springer-Verlag, Berlin, 1995.

Gierczak, T., R.K. Talukdar, J.B. Burkholder, R.W. Portmann, J.S. Daniel, S. Solomon, and A.R. Ravishankara, Atmospheric fate and greenhouse warming potentials of HFC-236fa and HFC-236ea, *J. Geophys. Res.*, *101*, 12905-12911, 1996.

Good, D.A., J.S. Francisco, A.K. Jain, and D.J. Wuebbles, Lifetimes and global warming potentials for dimethyl ethers and for fluorinated ethers: CH_3OCF_3 (E143a), CHF_2OCHF_2 (E134), CHF_2OCF_3 (E125), *J. Geophys. Res.*, in press, 1998.

Granier, C., J.-F. Müller, S. Madronich, and G.P. Brasseur, Possible causes for the 1990-1993 decrease in the global tropospheric CO abundances: A three-dimensional sensitivity study, *Atmos. Environ.*, *30*, 1673-1682, 1996.

Grossman, A.S., Grant, K.E., W.E. Blass, and D.J. Wuebbles, Radiative forcing calculations for CH_3Cl and CH_3Br, *J. Geophys. Res.*, *102*, 13651-13656, 1997.

Hansen, J., I. Fung, A. Lacis, D. Rind, S. Lebedeff, R. Ruedy, G. Russell, and P. Stone, Global climate changes as forecast by Goddard Institute for Space Studies 3-dimensional model, *J. Geophys. Res.*, *93*, 9341-9364, 1988.

Hansen, J., A. Lacis, R. Ruedy, M. Sato, and H. Wilson, How sensitive is the world's climate? *Res. Explor.*, *9*, 142-158, 1993.

Hansen, J., M. Sato, and R. Ruedy, Radiative forcing and climate response, *J. Geophys. Res.*, *102*, 6831-6864, 1997a.

Hansen, J., M. Sato, A. Lacis, and R. Ruedy, The missing climate forcing, *Philos. Trans. Roy. Soc. London B*, *352*, 231-240, 1997b.

Hansen, J., M. Sato, R. Ruedy, A. Lacis, K. Asamoah, K. Beckford, S. Borenstein, E. Brown, B. Cairns, B. Carlson, B. Curran, S. de Castro, L. Druyan, P. Etbarrow, T. Ferede, N. Fox, D. Gaffen, J. Glascoe, H. Gordon, S. Hollandsworth, X. Jiang, C. Johnson, N. Lawrence, J. Lean, J. Lerner, K. Lo, J. Logan, A. Luckett, M.P. McCormick, R. McPeters, R. Miller, P. Minnis, I. Ramberran, G. Russell, P. Russell, P. Stone, I. Tegen, S. Thomas, L. Thomason, A. Thompson, J. Wilder, R. Willson, and J. Zawodny, Forcing and chaos in interannual to decadal climate change, *J. Geophys. Res.*, *102*, 25679-25720, 1997c.

Hauglustaine, D.A., C. Granier, G.P. Brasseur, and G. Megie, The importance of atmospheric chemistry in the calculation of radiative forcing on the climate system, *J. Geophys. Res.*, *99*, 1173-1186, 1994.

Haywood, J.M., and V. Ramaswamy, Global sensitivity studies of the direct radiative forcing due to anthropogenic sulfate and black carbon aerosols, *J. Geophys. Res.*, *103*, 6043-6058, 1998.

Haywood, J.M., R.J. Stouffer, R.T. Wetherald, S. Manabe, and V. Ramaswamy, Transient response of a coupled model to estimated changes in greenhouse gas and sulfate concentrations, *Geophys. Res. Lett.*, *24*, 1335-1338, 1997.

Heathfield, A.E., C. Anastasi, J. Ballard, D.A. Newnham, and A. McCulloch, Integrated infrared absorption coefficients of CF_3OCF_2H and $CH_3OCF_2CF_2H$ at 297, 253, and 213 K, *J. Quant. Spectrosc. Radiat. Transfer*, *59*, 91-97, 1998a.

Heathfield, A.E., C. Anastasi, P. Pagsberg, and A. McCulloch, Atmospheric lifetimes of selected fluorinated ether compounds, *Atmos. Environ.*, *32*, 711-717, 1998b.

Heathfield, A.E., C. Anastasi, A. McCulloch, and F.M. Nicolaisen, Integrated infrared absorption coefficients of several partially fluorinated ether compounds: CF_3OCF_2H, CF_2HOCF_2H, $CH_3OCF_2CF_2H$, CH_3OCF_2CFClH, $CH_3CH_2OCF_2CF_2H$, $CF_3CH_2OCF_2CF_2H$, and $CH_2{=}CHCH_2OCF_2CF_2H$, *Atmos. Environ.*, *32*, 2825-2833, 1998c.

Imasu, R., A. Suga, and T. Matsuno, Radiative effects and halocarbon global warming potentials of replacement compounds for chlorofluorocarbons, *J. Meteorol. Soc. Japan*, *73*, 1123-1136, 1995.

IPCC (Intergovernmental Panel on Climate Change), *Climate Change: The IPCC Scientific Assessment*, edited by J.T. Houghton, B.A. Callander, and S.K. Varney, Cambridge University Press, Cambridge, U.K., 1990.

IPCC (Intergovernmental Panel on Climate Change), *Climate Change 1994: Radiative Forcing of Climate Change and An Evaluation of the IPCC IS92 Emission Scenarios*, edited by J.T. Houghton, L.G. Meira Filho, J. Bruce, H. Lee, B.A. Callander, N. Harris, A. Kattenberg, and K. Maskell, Cambridge University Press, Cambridge, U.K., 1995.

IPCC (Intergovernmental Panel on Climate Change), *Climate Change 1995: The Science of Climate Change*, edited by J.T. Houghton, L.G. Meira Filho, J. Bruce, H. Lee, B.A. Callander, E. Haites, N. Harris, and K. Maskell, Cambridge University Press, Cambridge, U.K., 1996.

Krol, M.C., and M. van Weele, Implications of variations in photodissociation rates for global tropospheric chemistry, *Atmos. Environ.*, *31*, 1257-1273, 1997.

Krol, M., P.J. van Leeuwen, and J. Lelieveld, Global OH trend inferred from methyl chloroform measurements, *J. Geophys. Res.*, *103*, 10697-10711, 1998.

Lacis, A.A., D.J. Wuebbles, and J.A. Logan, Radiative forcing by changes in the vertical distribution of ozone, *J. Geophys. Res.*, *95*, 9971-9981, 1990.

Lelieveld, J., and P.J. Crutzen, Indirect chemical effects of methane on climate warming, *Nature*, *355*, 339-342, 1992.

Lelieveld, J., and R. van Dorland, Ozone chemistry changes in the troposphere and consequent radiative forcing of climate, in *Atmospheric Ozone as a Climate Gas*, edited by W.-C. Wang and I.S.A. Isaksen, Springer-Verlag, Berlin, 1995.

Lelieveld, J., P.J. Crutzen, and F.J. Dentener, Changing concentration, lifetime, and climate forcing of atmospheric methane, *Tellus*, *50B*, 128-150, 1998.

Liu, S.C., and M. Trainer, Responses of tropospheric ozone and odd hydrogen radicals to column ozone changes, *J. Atmos. Chem.*, *6*, 221-233, 1988.

MacKay, R.M., M.K.W. Ko, R.L. Shia, Y. Yang, S. Zhou, and G. Molnar, An estimation of the climatic effects of the stratospheric ozone losses during the 1980s, *J. Clim.*, *10*, 774-788, 1997.

Madronich, S., and C. Granier, Tropospheric chemistry changes due to increased UV-B radiation, in *Stratospheric Ozone Depletion/UV-B Radiation in the Biosphere*, NATO ASI Series Vol. I 18, edited by R.H. Biggs and M.E.B. Joyne, Springer-Verlag, Berlin, 1994.

Marenco, A., H. Gouget, P. Nedelec, J.P. Pages, and F. Karcher, Evidence of a long-term increase in tropospheric ozone from Pic du Midi data series: Consequences, positive radiative forcing, *J. Geophys. Res.*, *99*, 16617-16632, 1994.

McDaniel, A.H., C.A. Cantrell, J.A. Davidson, R.E. Shetter, and J.G. Calvert, The temperature dependent infrared absorption cross-sections for the chlorofluorocarbons: CFC-11, CFC-12, CFC-13, CFC-14, CFC-22, CFC-113, CFC-114, and CFC-115, *J. Atmos. Chem.*, *12*, 211-227, 1991.

Mitchell, J.F.B., T.C. Johns, J.M. Gregory, and S.F.B. Tett, Climate response to increasing levels of greenhouse gases and sulphate aerosols, *Nature*, *376*, 501-504, 1995.

Molina, L.T., P.J. Wooldridge, and M.J. Molina, Atmospheric reactions and ultraviolet and infrared absorptivities of nitrogen trifluoride, *Geophys. Res. Lett.*, *22*, 1873-1876, 1995.

Molnar, G.I., M.K.W. Ko, S. Zhou, and N.-D. Sze, Climatic consequences of observed ozone loss in the 1980s: Relevance to the greenhouse problem, *J. Geophys. Res.*, *99*, 25755-25760, 1994.

Myhre, G., and F. Stordal, Role of spatial and temporal variations in the computation of radiative forcing and GWP, *J. Geophys. Res.*, *102*, 11181-11200, 1997.

Myhre, G., F. Stordal, B. Rognerud, and I.S.A. Isaksen, Radiative forcing due to stratospheric ozone, in *Atmospheric Ozone: Proceedings of the XVIII Quadrennial Ozone Symposium*, edited by R.D. Bojkov and G. Visconti, L'Aquila, Italy, Parco Scientifico e Technologico d'Abruzzo, pp. 813-816, 1998a.

Myhre, G., E.J. Highwood, K.P. Shine, and F. Stordal, New estimates of radiative forcing due to well mixed greenhouse gases, *Geophys. Res. Lett.*, *25*, 2715-2718, 1998b.

Newnham, D., and J. Ballard, Fourier transform infrared spectroscopy of HCFC-142b vapour, *J. Quant. Spectrosc. Radiat. Transfer*, *53*, 471-479, 1995.

Newnham, D., J. Ballard, and M. Page, Infrared band strengths of HFC-134a vapour, *J. Quant. Spectrosc. Radiat. Transfer*, *55*, 373-381, 1996.

Novelli, P.C., K.A. Masarie, P.P. Tans, and P.M. Lang, Recent changes in atmospheric carbon monoxide, *Science*, *263*, 1587-1590, 1994.

Pappasavva, S., S. Tai, K.H. Illinger, and J.E. Kenny, Infrared radiative forcing of CFC substitutes and their atmospheric reaction products, *J. Geophys. Res.*, *102*, 13643-13650, 1997.

Pinnock, S., and K.P. Shine, The effects of changes in HITRAN and uncertainties in the spectroscopy on infrared irradiance calculations, *J. Atmos. Sci.*, *55*, 1950-1964, 1998.

Pinnock, S., M.D. Hurley, K.P. Shine, T.J. Wallington, and T.J. Smyth, Radiative forcing by hydrochlorofluorocarbons and hydrofluorocarbons, *J. Geophys. Res.*, *100*, 23227-23238, 1995.

Portmann, R.W., S. Solomon, J. Fishman, J.R. Olson, J.T. Kiehl, and B. Briegleb, Radiative forcing of the Earth-climate system due to tropical tropospheric ozone production, *J. Geophys. Res.*, *102*, 9409-9417, 1997.

Prather, M.J., Lifetimes and eigenstates in atmospheric chemistry, *Geophys. Res. Lett.*, *21*, 801-804, 1994.

Prather, M.J., Time scales in atmospheric chemistry: Theory, GWPs for CH_4 and CO, and runaway growth, *Geophys. Res. Lett.*, *23*, 2597-2600, 1996.

Prather, M.J., and C.M. Spivakovsky, Tropospheric OH and the lifetimes of hydrochlorofluorocarbons, *J. Geophys. Res.*, *95*, 18723-18729, 1990.

Prinn, R.G., R.F. Weiss, B.R. Miller, J. Huang, F.N. Alyea, D.M. Cunnold, P.J. Fraser, D.E. Hartley, and P.G. Simmonds, Atmospheric trends and lifetime of CH_3CCl_3 and global OH concentrations, *Science*, *269*, 187-192, 1995.

Ramaswamy, V., and C.T. Chen, Climate forcing-response relationships for greenhouse and shortwave radiative perturbations, *Geophys. Res. Lett.*, *24*, 667-670, 1997.

Ramaswamy, V., M.D. Schwarzkopf, and K.P. Shine, Radiative forcing of climate from halocarbon-induced global stratospheric ozone loss, *Nature*, *355*, 810-812, 1992.

Rodhe, H., and P. Crutzen, Climate and CCN, *Nature*, *375*, 111, 1995.

Roehl, C.M., D. Boglu, C. Brühl, and H.K. Moortgat, Infrared band intensities and global warming potentials of CF_4, C_2F_6, C_3F_8, C_4F_{10}, C_5F_{12}, and C_6F_{14}, *Geophys. Res. Lett.*, *22*, 815-818, 1995.

Roelofs, G.-J., J. Lelieveld, and R. van Dorland, A three dimensional chemistry/general circulation model simulation of anthropogenically derived ozone in the troposphere and its radiative climate forcing, *J. Geophys. Res.*, *102*, 23389-23401, 1997.

Rothman, L.S., R.R. Gamache, R.H. Tipping, C.P. Rinsland, M.A.H. Smith, D.C. Benner, V.M. Devi, J.M. Flaud, C. Camy-Peyret, A. Perrin, A. Goldman, S.T. Massie, L.R. Brown, and R.A. Toth, The HITRAN molecular database: Editions of 1991 and 1992, *J. Quant. Spectrosc. Radiat. Transfer*, *48*, 469-507, 1992.

Santer, B.D., K.E. Taylor, T.M.L. Wigley, T.C. Johns, P.D. Jones, D.J. Karoly, J.F.B. Mitchell, A.H. Oort, J.E. Penner, V. Ramaswamy, M.D. Schwarzkopf, R.J. Stouffer, and S. Tett, A search for human influences on the thermal structure of the atmosphere, *Nature*, *382*, 39-46, 1996.

Schnell, R.C., S.C. Liu, S.J. Oltmans, R.S. Stone, D.J. Hofmann, E.G. Dutton, T. Deshler, W.T. Sturges, J.W. Harder, S.D. Sewell, M. Trainer, and J.M. Harris, Decrease of summer tropospheric ozone concentrations in Antarctica, *Nature*, *351*, 726-729, 1991.

Shetter, R.E., C.A. Cantrell, K.O. Lantz, S.J. Flocke, J.J. Orlando, G.S. Tyndall, T.M. Gilpin, C.A. Fischer, S. Madronich, and J.C. Calvert, Actinometric and radiometric measurements and modeling of the photolysis rate coefficient of ozone to $O(^1D)$ during Mauna Loa Observatory Photochemistry Experiment 2, *J. Geophys. Res.*, *101*, 14631-14641, 1996.

Shine, K.P., R.S. Freckleton, and P.M. de F. Forster, Comment on "Climate forcing by stratospheric ozone depletion calculated from observed temperature trends," *Geophys. Res. Lett.*, *25*, 663-664, 1998.

Sigg, A., and A. Neftel, Evidence for a 50% increase in H_2O_2 over the past 200 years from a Greenland ice core, *Nature*, *351*, 557-559, 1991.

Sinha, A., and R. Toumi, A comparison of climate forcings due to chlorofluorocarbons and carbon monoxide, *Geophys. Res. Lett.*, *23*, 65-68, 1996.

Smith, K., D. Newnham, M. Page, J. Ballard, and G. Duxbury, Infrared band strengths and absorption cross-sections of HFC-32 vapour, *J. Quant. Spectrosc. Radiat. Transfer*, *56*, 73-82, 1996.

Solomon, S., and J.S. Daniel, Impact of the Montreal Protocol and its Amendments on the rate of change of global radiative forcing, *Clim. Change*, *32*, 7-17, 1996.

Takahashi, K., Y. Matsumi, and M. Kawasaki, Photodissociation processes of ozone in the Huggins band at 308-326 nm: Direct observation of $O(^1D_2)$ and $O(^3P_j)$ products, *J. Phys. Chem.*, *100*, 4084-4089, 1996.

Tegen, I., P. Hollrig, M. Chin, I. Fung, D. Jacob, and J. Penner, Contribution of different aerosol species to the global aerosol extinction optical thickness: Estimates from model results, *J. Geophys. Res.*, *102*, 23895-23915, 1997.

Tett, S.F.B., J.F.B. Mitchell, D.E. Parker, and M.R. Allen, Human influence on the atmospheric vertical temperature structure: Detection and observations, *Science*, *274*, 1170-1173, 1996.

Thompson, A.M., M.A. Huntley, and R.W. Stewart, Perturbations to tropospheric oxidants, 1985-2035, *J. Geophys. Res.*, *95*, 9829-9844, 1990.

Toumi, R., S. Bekki, and K.S. Law, Indirect influence of ozone depletion on climate forcing by clouds, *Nature*, *372*, 348-351, 1994.

Toumi, R., S. Bekki, and K.S. Law, Response to climate and CCN by Rodhe and Crutzen, *Nature*, *375*, 111, 1995.

Trolier, M., and J.R. Wiesenfeld, Relative quantum yield of $O(^1D_2)$ following photolysis between 275 and 325 nm, *J. Geophys. Res.*, *93*, 7119-7124, 1988.

Van Dop, H., and M. Krol, Changing trends in tropospheric methane and carbon monoxide: A sensitivity analysis of the OH-radical, *J. Atmos. Chem.*, *25*, 271-288, 1996.

van Dorland, R., F.J. Dentener, and J. Lelieveld, Radiative forcing due to tropospheric ozone and sulfate aerosols, *J. Geophys. Res.*, *102*, 28079-28100, 1997.

Varanasi, P., Z. Li, V. Nemtchinov, and A. Cherukuri, Spectral absorption coefficient data on HCFC-22 and SF_6 for remote sensing application, *J. Quant. Spectrosc. Radiat. Transfer*, *52*, 323-332, 1994.

Wallington, T.J., W.F. Schneider, J. Sehested, M. Bilde, J. Platz, O.J. Nielsen, L.K. Christensen, M.J. Molina, L.T. Molina, and P.W. Wooldridge, Atmospheric chemistry of HFE-7100 ($C_4F_9OCH_3$): Reaction with OH radicals, UV spectra, and kinetic data for $C_4F_9OCH_2\cdot$ and $C_4F_9OCH_2O_2\cdot$ radicals and the atmospheric fate of $C_4F_9OCH_2O\cdot$ radicals, *J. Phys. Chem. A.*, *101*, 8264-8274, 1997.

Wang, W.-C., J.P. Pinto, and Y.L. Yung, Climatic effects due to halogenated compounds in the Earth's atmosphere, *J. Atmos. Sci.*, *37*, 333-338, 1980.

Wild, O., O.V. Rattigan, R.L. Jones, J.A. Pyle, and R.A. Cox, 2-Dimensional modeling of some CFC replacement compounds, *J. Atmos. Chem.*, *25*, 167-199, 1996.

WMO (World Meteorological Organization), *Scientific Assessment of Ozone Depletion: 1991*, Global Ozone Research and Monitoring Project—Report No. 25, Geneva, 1992.

WMO (World Meteorological Organization), *Scientific Assessment of Ozone Depletion: 1994*, Global Ozone Research and Monitoring Project—Report No. 37, Geneva, 1995.

Zhong, W., R. Toumi, and J.D. Haigh, Climate forcing by stratospheric ozone depletion calculated from observed temperature trends, *Geophys. Res. Lett.*, *23*, 3183-3186, 1996.